Additive manufacturing high performance graphene-based composites

LI, Yan ; FENG, Zuying; HUANG, Lijing; Essa, Khamis; BILOTTI, Emiliano; ZHANG, Han; PEIJS, Ton; HAO, Liang

DOI:
10.1016/j.compositesa.2019.105483

Review

Additive Manufacturing High Performance Graphene-based Composites: A Review

Yan Li, Zuying Feng, Lijing Huang, Khamis Essa, Emiliano Bilotti, Han Zhang, Ton Peijs, Liang Hao

PII: S1359-835X(19)30232-5
DOI: https://doi.org/10.1016/j.compositesa.2019.105483
Article Number: 105483
Reference: JCOMA 105483

To appear in: *Composites: Part A*

Received Date: 17 October 2018
Revised Date: 24 May 2019
Accepted Date: 10 June 2019

Please cite this article as: Li, Y., Feng, Z., Huang, L., Essa, K., Bilotti, E., Zhang, H., Peijs, T., Hao, L., Additive Manufacturing High Performance Graphene-based Composites: A Review, *Composites: Part A* (2019), doi: https://doi.org/10.1016/j.compositesa.2019.105483

Additive Manufacturing High Performance Graphene-based Composites: A Review

Yan LI[1], Zuying FENG[2]*, Lijing HUANG[2], Khamis ESSA[3], Emiliano BILOTTI[4], Han ZHANG[4], Ton PEIJS[5], Liang HAO[1]*

[1] Gemmological Institute, China University of Geosciences, Wuhan, 430074, P. R. China.

[2] Engineering Research Centre of Nano-Geomaterials of Ministry of Education, Faculty of Materials Science and Chemistry, China University of Geosciences, Wuhan 430074, P. R. China.

[3] Mechanical Engineering, University of Birmingham, Birmingham, B15 2TT, UK

[4] School of Engineering and Materials Science, Queen Mary University of London, Mile End Road, London, E1 4NS, UK

[5] Materials Engineering Centre, WMG, University of Warwick, Coventry, CV4 7A, UK

Corresponding authors: fengzuying@163.com; liang_hao1972@foxmail.com

GRAPHIC ABSTRACT

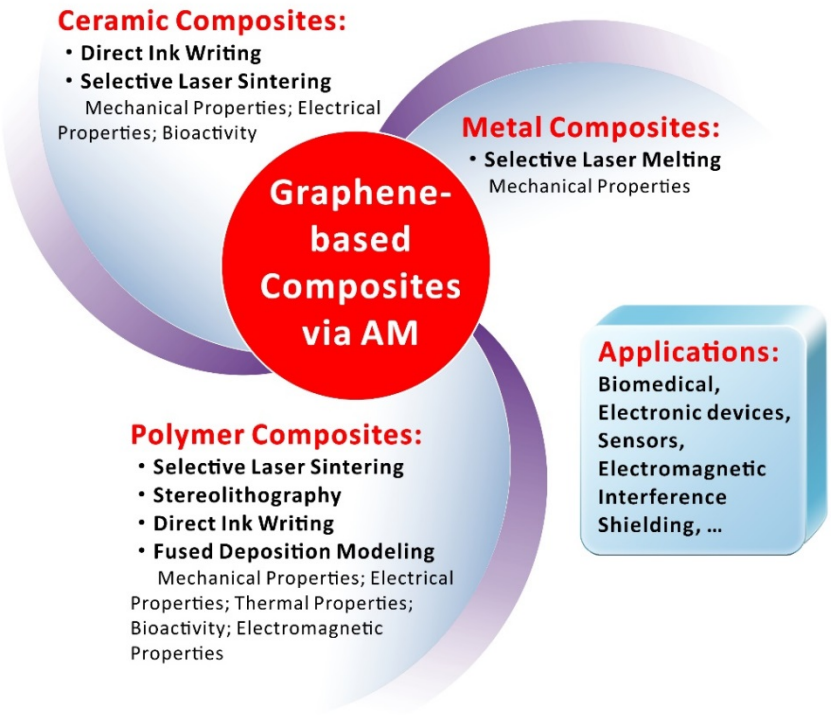

ABSTRACT

The unique physical properties of graphene and its composites, combined with the capability of additive manufacturing (AM), to net shape manufacture intricate 3D objects layer-by-layer, promise to open up a plethora of new opportunities and challenges. In this review, we provide a comprehensive overview of graphene-based ceramic, metal, and polymer composites, produced by a variety of AM methods. It will be shown that the multifunctional properties and potential capabilities of graphene-based composites can be uniquely exploited by the use of AM technologies, enabling novel applications in fields like biomedicine, energy, sensing and electromagnetic interference (EMI) shielding.

Keywords: *graphene; additive manufacturing; nanocomposites; mechanical properties; electrical properties; tissue engineering*

1. Introduction

1.1. Graphene and Derivatives Properties.

Graphene, a two-dimensional (2D) nano-scale material, has attracted great interest from academia and industries since Andre Geim and Konstantin Novoselov firstly isolated graphene from natural graphite [1, 2]. Graphene is a monolayer of sp^2 hybridized carbon atoms, tightly packed in a 2D honeycomb lattice (crystalline structure) [3] with excellent optical properties (only 2.3% light absorption over a broad range of wavelengths), high surface area (2630 m^2/g) [4, 5], high mechanical properties (e.g., Young's modulus 1 TPa, tensile strength 130 GPa, respectively [6]), superior thermal conductivity (~ 5000W/mk) [7-9], excellent intrinsic mobility ($2x10^5$ cm^2/sv, room temperature) [10]and barrier properties (impermeable to most liquids and gases) [11]. Typically, graphene is synthesized by chemical vapour deposition (CVD), mechanical and electrochemical exfoliation methods [12-15]. Single layer graphene (SLG) is difficult to manufacture in large-scale as well as difficult to disperse in a solution or isolated in gas phase due to its large specific surface area. Thus, graphene related materials such as multi-layer graphene (MLG), graphene nanoplatelets (GNP) or graphene oxides (GO) are much more frequently studied due to their availability. The oxidized functional groups of GO can enhance the dispersion of graphene into a matrix phases, and minimise phase

separation and aggregation of graphene. However, the presence of such functional groups will deteriorate the electrical conductivity of GO due to the extensive presence of sp^3 C-C bonds as well as defects (disruption of the basal graphitic layer) and functional groups. Retrieval of electrical conductivity can however be achieved, at least partially, by restoration of the sp^2 bonds. Reduced GO (rGO) is obtained by the chemical or physical reduction of GO, which is a cost-effective strategy to prepare graphene sheets with good electrical properties. As an excellent candidate nanofiller, the performance of graphene-based composites promises huge improvements compared to the unfilled matrix material. Ren *et al.* [16] reported that the electrical conductivity of 5 wt.% graphene nanosheets/cyanate ester nanocomposite was increased from 10^{-12} to 4.59 Sm^{-1} compared to neat cyanate ester. Owing to the formation of the efficient 3D electric and thermally conductive pathways, the electromagnetic interference (EMI) shielding effectiveness and thermal conductivity of the resulting nanocomposite reach a maximum value of 38 dB and 1.18 Wm^{-1} K^{-1}, respectively, which have great potential to be used in advanced electronic packaging. Pavithra *et al.* [17] reported Cu-Graphene composites with a hardness as high as 2.5 GPa and an elastic modulus of 137 GPa. In addition, these materials had also comparable electrical conductivity to that of pure copper. Porwal *et al.* [18] reported that graphene reinforced Al_2O_3 ceramic composites exhibited a 40% increase in fracture toughness. Very recently, the network formation of graphene nanofillers in epoxy resins has also been studied and visualised, as its effect on multifunctional properties like strain sensing and Joule heating [19].

In recent years, the use of graphene has been applied to a variety of fields, including optoelectronics, energy storage, electronics as well as biomedical applications [20-24]. In many of these fields, the control of an appropriate macroscopic and microscopic structure is often of paramount importance, if not the limiting factor, in order to satisfy stringent and often contrasting technical requirements. The possibility of creating sophisticated and precise three-dimensional (3D) structures, including hierarchical and gradient structures, via additive manufacturing (AM) technologies, might be the missing link to unlock the potential of graphene-based composites and impact a number of application fields.

1.2. Additive Manufacturing Methods for Graphene-based Composites

AM is sometimes also termed as three-dimensional printing (3DP), rapid prototyping (RP),

solid freeform fabrication (SFF), or layered manufacturing (LM). During the process of AM, a computer-aided design (CAD) software is utilized to build a 3D model object. A wide range of materials, such as metals, polymers, ceramics or even concrete, can be successfully transformed into products using AM [25, 26]. There are striking features that distinguish AM from other conventional manufacturing (CM) methods. Notably, AM can directly manufacture 3D complicated final objects, without any mould and without any intermediate steps, like joining or assembling. Although significant progress has been achieved in the development of 2D structure with graphene, the manufacturing of 3D multifunctional graphene composites structures still remains a challenge. A variety of traditional methods such as direct-writing, soft-lithography and photolithography have been utilized to produce 2D structured graphene composites successfully. However, inevitable drawbacks of these CM methods (such as extra etching processes, limitation on the choice of suitable substrates, high operational cost and high defect density in the developing object) hinder the development of graphene-based composites. Clearly, there is a promising potential for the combination of AM and graphene-based composites to open up new engineering prospects from energy storage to sensing, electromagnetic shielding or structural, and functional analytical devices. This is particularly the case if we hope to create composite materials with the same level of hierarchical structurization as natural composite materials like bone, wood or sea shells.

Multi-structured graphene-based composites produced via AM have many merits. With the aid of computer aided design or optimization, components or products are reproducible and can be precisely fabricated with highly complex architectures in high resolution, meeting various end-user requirements. Besides, AM processes are highly efficient (ranging from few minutes to several hours depending on the size and complexity of the specific printed component) and are relatively low cost. For instance, AM can manufacture scaffolds tissue engineering with highly advanced design porosities, pore size distributions, pore shape and controllable pore interconnectivity, which can bring superior mechanical properties and cell-seeding efficiency [27]. Chen *et al.* [28] prepared 3D thermoplastic polyurethane (TPU)/polylactic acid (PLA)/GO nanocomposites with 3D structures via an AM method which exhibited excellent biocompatibility, cell seeding, viability and mobility. The TPU/PLA with 0.5 wt.% GO exhibited the highest density of cells among all loadings of GO as well as compared to the TPU/PLA reference.

1.3. Aim of this Review

This review aims to provide a comprehensive and systematic summary of the current state of the art of graphene-based ceramic, metal and polymer composites fabricated via AM. Emphasis will be on four different AM methods to produce graphene-based polymer matrix composites (GPMCs) including its biomedical, electronic, sensing and electromagnetic shielding applications (**Fig.1**).

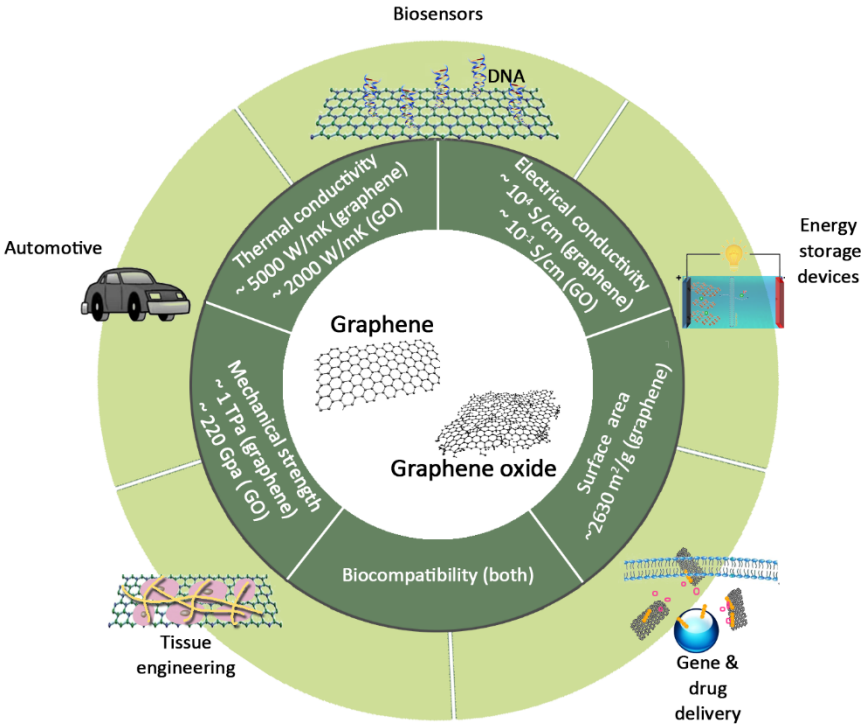

Fig. 1 Schematic overview of various potential applications corresponding to different properties of graphene and GO.

2. Conventional Processing Methods for Graphene-based Composites

Because of the great interest in graphene related materials, there are a number of mature and conventional processing methods have been used to prepare graphene-based composites. This section summarizes the most representative conventional methods for graphene-based composites, typically in the form of simple structures like films, hydrogels, powders or bulk graphene-based materials. These are partially relevant for AM, as they

provide a way to prepare graphene composite materials that can then be used in AM. AM methods allow the production of graphene-based composites with 3D network architectures and tailored morphologies. However, one distinct requirement for all AM methods, different from conventional methods, is the flowability of the used material. The developed graphene-based material must be in liquid, powder or another flowable form when they are processed by 3D printing. Moreover, rapid solidification (either physically and/or chemically) is important to preserve the desired structures.

2.1. Graphene–based Ceramic Matrix Composites (GCMCs) Processing Methods

The properties of graphene-based ceramic matrix composites (GCMCs) depend on the quality of the graphene, the dispersion of the graphene nanosheets in the ceramic matrix and the retention of the graphene structure at high sintering temperatures [29]. Many scientists have found processing routes for preparing well dispersed graphene in a ceramic matrix such as akermanite/graphene [30], Al_2O_3/graphene [31-33], SiO_2/graphene [34, 35], silicon carbide (SiC)/graphene [36] and titanium carbide/graphene [37]. These synthesis methods are briefly introduced below.

Powder processing is commonly used for the processing of ceramic matrix composites with various matrix materials being used including alumina, silicon nitride, zirconia, and silica. In this process, the fillers can be dispersed by ultrasonication or ball milling with ceramic powders [31, 36, 38]. Sol-gel processing requires creating a precursor that can endure condensation to prepare a medium to homogeneously dispersed graphene suspension. Typically, a uniformly dispersed sol is obtained by sonicating a well dispersed graphene suspension incorporating tetramethyl orthosilicate. Then a catalyst like acidic water will be added to promote hydrolysis, forming composite gels after condensation at room temperature [37]. Colloidal particles with opposite surface charges attract each other and automatically assemble and settle down to form uniform powders [39]. The key to this process is to obtain a uniform dispersing medium when mixing [32, 40].

High temperature sintering is an essential and critical processing step in ceramic matrix composite preparation. Among all the sintering techniques for ceramic matrix composites (e.g., hot pressing, hot isostatic pressing, spark plasma sintering (SPS), and microwave sintering, etc. [31, 41-44]), over 90% of graphene-ceramic composites are prepared by SPS

with advantages such as: a) a fast heating rate increases the sintering efficiency and avoids grain growth and degradation of the graphene structure; b) hot sintering at maximum pressure, which is greatly beneficial to improving the density of the ceramic matrix composites and reducing the sintering temperature [39]; and c) *in-situ* reduction of GO to graphene during sintering at high temperatures [45].

Nevertheless, SPS can not satisfy the need of some applications, such as graphene-reinforced bioceramic scaffolds, which require precise control of 3D complex structure [46]. AM methods like direct ink writing (DIW) are suitable alternatives to fabricate customized shapes with interconnected porous 3D structure, achieving great control over degree of porosity, pore size and connectivity. However, additional cares must be taken for high-concentrated ceramic inks, including viscoelastic and pseudo-plastic behaviour to flow out of the nozzle as well as the capacity to retain the cylindrical shape.

2.2. Graphene–based Metal Matrix Composites (GMMCs) Processing Methods

Graphene-based metal composites (GMMCs) usually exhibit higher strength and Young's modulus than that of pure metal materials. Right now, there are some relatively mature methods for the preparation of GMMCs including mechanical mixing, chemical synthesis, electrodeposition and self-assembly approach. Mechanical mixing is a method using physical force to mix graphene and metal. For example, in a method like friction stir processing, the metallic materials are usually softened by the frictional heat generated through mechanical stirring of a rotating tool [47-50]. Chemical synthesis, including *in-situ* synthesis, hydrothermal preparation and even molecular-level mixing (MLM), is a method to prepare nanocomposites through the reduction of GO and metal salts [51, 52]. Recently, MLM, a newly emerging fabrication process, is feasible to make homogeneous dispersion of rGO and stronger interfacial bonding between rGO and metal matrix (e.g., Cu, Co, Ni) [52, 53] with excellent mechanical properties (for instance, 1.5 wt.% rGO/Ni composite demonstrated a 95.2 % increase in tensile strength and a 327.6% increase in yield strength [52]).

Electrodeposition is a simple, cost-effective and scalable method. It not only preserves the original properties of graphene or other filler materials but also incorporates these properties in composite structures [54]. The quality of these composites is influenced by many operating parameters, such as current density, electrolyte composition and bath agitation, etc. Besides,

it is also possible to fabricate a wide range of pure metal or alloy coatings on such composites. Li *et al.* [17, 55] used pulse-reverse electrodeposition (**Fig.2**) to prepare homogeneously dispersed graphene reinforced Ni composites with high graphene filler content. However, the electrodeposition method still exhibits some deficiencies such as a long reduction period, poor controllability and single material structure [56, 57].

Self-assembly approach, a methodology to synthesise the GMMCs, is used to compound the graphene dispersion and metallic materials (Al, Cu) firstly, and then assemble the graphene sheets with the metal matrix through electrostatic attraction, covalent or uncovalent bonding to form the ultra-dense macrostructures [58-60] (e.g., self-assembly Al and Bi_2O_3 on the graphene sheets with ultradense macrostructures [58]). Compared with the chemical synthesis, self-assembly approach fabricates the GMMCs with simpler controllable particle size and more highly uniform dispersion of graphene nanocomposites.

Generally, AM methods can manufacture GMMCs without time- and energy-consuming post-processing steps such as hot shaping or machining, which are essential for conventionally manufactured GMMCs. Laser-based AM method is one of the most common methods used to fabricate GMMCs. It generally requires the use of graphene/metal powders which possess appropriate particle size distributions and excellent flowability. Using high energy ball milling to mix graphene with metallic matrix causes severe plastic deformation and, as a consequence, poor flowability for metal matrix powders. Alternative milder techniques to prepare metal powder containing graphene for AM are necessary. Lin *et al.* [61] used poly(vinyl alcohol) (PVA) to disperse GO. The evaporation of the solution caused by the laser helps the alignment of GOs and thus preventing aggregation. Other parameters, including deposition rate, beam size, process temperature, scanning strategy, have an obvious influence on the microstructure of 3D GMMCs objects manufactured by laser-based AM techniques. Thermal gradients are easily created during the high temperature laser processing and the resulting large tensile residual stress and deformations must be taken in consideration.

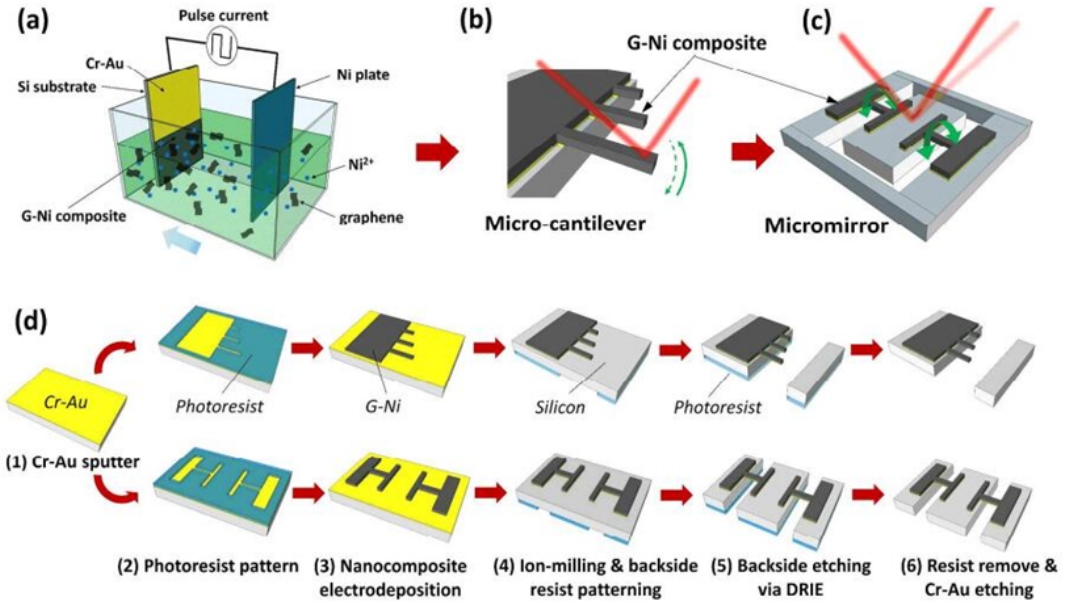

Fig. 2 Schematic illustration of the strategy for pulse-reverse electrodeposition*. A micro-patterned graphene-Ni composite was; (a) electrodeposited onto Si substrate via a pulse-reverse electrodeposition method; (b) the graphene -Ni composite microcantilever arrays and (c) micromirrors were fabricated and resonant vibrated for evaluating Young's modulus and resistance to plastic deformation under dynamic conditions, respectively; (d) the fabrication process of these composite microstructures. Reprinted with permission from [55]. Copyright 2016 American Chemical Society.*

2.3. Graphene–based Polymer Matrix Composites (GPMCs) Processing Methods

The preparation and properties of GPMCs have recently been reviewed in detail by a number of researchers [62-68]. Most of the published works use GO, which can be obtained in large scale, for exfoliation and dispersion in different polymer matrices. The functional groups present onto GO allow a strong interfacial bond filler/matrix. However, the ultra-thin individual GO nanosheets easily crumble and wrinkle and have significantly inferior electrical, thermal and mechanical properties compared to graphene. Three main strategies for synthesizing GPMCs are: *in-situ* polymerization, solution mixing, and melt compounding.

As for the *in-situ* polymerization technique, graphene, modified graphene or graphite nanoplatelets, is first swollen within a liquid monomer. Polymerization is initiated either by radiation or heating after a suitable initiator is diffused in the liquid monomer [69, 70]. A variety of graphene-based polymer nanocomposites have been manufactured through the *in-*

situ polymerization, such as polystyrene (PS)/graphene [70], poly(methyl methacrylate) (PMMA)/expanded graphite (EG) [71], nylon-6 (PA6)/graphene [72] and poly(vinylidene fluoride) (PVDF)/PMMA/graphene [73] etc. However, *in-situ* polymerization is not an economically attractive and scalable method for dispersing nanoparticles into polymers compared to solution or melt compounding methods [62].

Solution intercalation method is performed in a solvent system where the polymer or pre-polymer is compatible and solubilized. Graphene or modified graphene can be dispersed into a suitable solvent, such as acetone, toluene, tetrahydrofuran (THF), chloroform or dimethylformamide (DMF) owing to the weak forces that hold the layers together [66]. The polymer then adsorbs onto the delaminated graphene sheets. When the solvent is evaporated, the sheets will assemble with the polymer to form a nanocomposite. This method allows even polymers with low or no polarity to create intercalated nanocomposites. The driving force for polymer intercalation from solution into graphene is the entropy gained by the desorption of solvent molecules, compensating for the decrease in conformational entropy of the intercalated polymer chains [74]. However, the thorough removal of the solvent is an important issue, significantly influencing the final physical properties [75]. A variety of polymer nanocomposites have been reported using this method, such as polyethylene grafted PVA/graphene, polyimide (PI)/graphene [76] and PVDF/graphene [77] have all been prepared using this method.

Melt compounding method is a solvent-free method for the preparation of thermoplastic nanocomposites, popular because of its simplicity and its compliance with large-scale industrial production. Graphene related materials such as graphene, GO or modified graphene are directly mixed with a thermoplastic polymer melt. This usually involves mechanical mixing using conventional methods like extrusion compounding in a twin-screw extruder at temperatures well above the melting or softening temperatures of the polymer matrix. Nanocomposites are formed via the intercalation of polymer chains and/or exfoliation of graphene related materials. Some polymers which are not suitable for *in-situ* polymerization or solution processing can be processed through melt compounding. A variety of polymer nanocomposites have been prepared using this method such as polypropylene (PP)/graphene [78], high-density polyethylene (HDPE)/EG [79], PA6/EG [80], PLA/GNP [81], etc.

Besides using these techniques on their own, some polymer/graphene composites have been prepared by combining *in-situ* polymerization, solution compounding with one or more other procedures such as melt blending, shear mixing and/or master batch blending, etc. A combination of techniques can for instance become necessary when the system viscosity increases rapidly with solvent reduction, as in the case of epoxy matrix. The approach of combining different methods has been adopted an improved dispersion of nanofillers in different matrices [82, 83]. It can be a promising approach, as it can mitigate problems of each individual technique while optimising the advantages.

The above mentioned conventional methods are the ones also used to prepare graphene nanocomposites to then feed AM. Previous studies have examined graphene-based polymer materials for AM methods, prepared via *in-situ* polymerization, solution compounding, and melt compounding. Solution mixing is the most common method used to prepare polymer/graphene mixtures with solvents like ethanol [84], chloroform [85] and acetone [86], which are frequently used for their relatively low boiling points. A quick evaporation of the resulting solutions or dispersions after printing is necessary to retain the shape of the 3D object after printing.

Various AM methods have been applied to produce graphene-based polymer composites, each with bespoke requirements. Fused deposition modelling (FDM) demands materials to be processed by extrusion into filament with a relatively uniform diameter. Homogeneously distributed graphene/polymer powders are required in powder bed based AM methods and liquid light curable graphene-based resin is required for vat polymerization printing methods. Moreover, AM methods such as stereolithography can achieve 3D structured graphene-based photocurable resins, while conventional methods can only produce 2D films.

Table 1 The representative synthetic methods for graphene-based composites and their characteristics

Matrix	Techniques	Characteristics	Materials	Advantages and disadvantages	Ref.
Ceramic	Power processing	Ball milling or planetary ball milling	Alumina, silicon, nitride, zirconia, and silica	● Producing well dispersed graphene–ceramic composites ● Possible damage and degradation of graphene	[31, 33-36, 38]
	Sol-Gel processing	Creating a precursor	TiOC	● Easy for doped materials ● Easy for dispersed composites to dissolve and disperse in a liquid phase	[37, 40]
	Colloidal processing	Producing a dispersion of graphene and ceramics to produce composites based on colloidal chemistry.	Al_2O_3, Si_2N_3	● Difficult to evaluate dispersion homogeneity ● Lack of quantitative information of graphene and ceramic matrix	[31, 39, 41-43]
Metal	Chemical synthesis	Hydrothermal preparation, the reduction of GO and metal salt	Cu, Co, Ni and other metal materials	● Limited by complex procedure, high temperature, high cost, and many parameters during the reaction	[47-50]
	Mechanical mixing	Physical force to mix graphene and metal	Mg, Al, Sn	● Risk of damage of the structure of graphene during stirring	[87-89]
	Electrodeposition	Using electric current to reduce dissolved metal cations and form a coherent metal coating on an electrode	Pure metal and alloy	● Controlled by e electronic parameters ● Matrix materials are limited ● Thickness of the coating is thin	[17, 54-57]
	Self-assembly approach	Assembly fabricated with electrostatic attraction, covalent or uncovalent bonding	Al, Cu	● Simpler controllable particle size ad more highly uniform dispersion of graphene nanocomposites	[58-60]
Polymer	*In-situ* polymerization	Adding a suitable initiator to make liquid monomer polymerize	PS, PMMA, PA6 and PVDF/PMMA	● Not an economically attractive and scalable method	[69-73]
	Solution compounding	Dispersed in suitable solvent system, adsorbing onto the delaminated graphene sheets and creating the nanocomposite by evaporating solvent	PE-g-MA, PVA/graphene, PVC, and PMMA/silica	● Difficult to remove the solvent residue	[66, 74, 75]
	Melt compounding	High–shear mixing of graphene and molten thermoplastic polymer matrix	PP/graphene, HDPE/EG, PA6/EG, PLA/EG	● Suitable for some specific polymers which can not be processed by *in-situ* polymerization or solution method ● Easily adapted by industry	[78-81]

3. AM Methods for Graphene-based Composites

According to the ISO/ASTM standard 52900:2015 [90], current AM methods are classified into seven categories, including direct energy deposition, power bed fusion, vat polymerization, materials jetting, materials extrusion, sheet lamination, and binder jetting. The main four types of AM methods, usually used with graphene-based composites, are summarized and compared in **Table 2**.

Table 2 A summary of AM methods for graphene-based composites from literature (until 2019).

Matrix	Powder bed fusion	Vat polymerization	Materials extrusion	Binder jetting
GCMC	√	×	√	×
GMMC	√	×	×	√
GPMC	√	√	√	×

3.1. Powder Bed Fusion

Power bed fusion (PBF), including direct metal laser sintering (DMLS), electron beam melting (EBM), selective laser sintering (SLS) and selective laser melting (SLM), is an AM process which utilizes thermal energy to selectively melt or sinter certain molten areas/pools of a powder bed [91, 92]. Among those mentioned techniques, SLS was found to successfully manufacture graphene-based ceramic (Al_4C_3 [93]), metal (Fe/GO [61], Al/graphene [94], Cu/graphene [95]) and polymer/graphene composites [96, 97]. SLS uses a laser which selectively scans a powder bed, forming 2D patterns of fused material by the heat of the laser [98]. Objects are built layer-by-layer by repeatedly laying down a new layer of powder upon a solidified layer (**Fig.3a**). Factors like laser power, energy density, powder particle size distribution, scan speed, and scan strategy can determine the printing resolution of SLS [99-101].

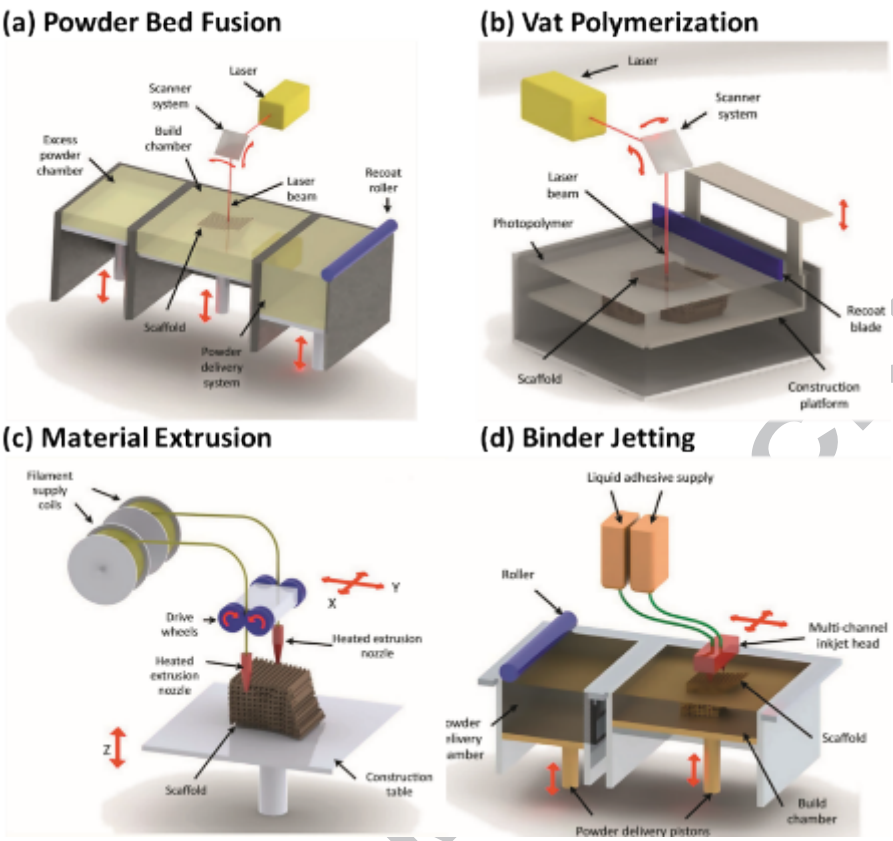

Fig. 3 Schematic diagram of the typical AM techniques for graphene-based composites (a) PDF; (b) vat polymerization; (c) material extrusion and (d) binder jetting. Reprinted with permission from [102]. Copyright 2017 Elsevier.

3.2. Vat Polymerization

Vat photopolymerization fabricates objects by solidifying liquid photosensitive resin with ultraviolet (UV) light (**Fig.3b**). Vat polymerization covers the following systems such as stereolithography apparatus (SLA), digital light processing (DLP), scan, spin and selectively photocure (3SP), and continuous liquid interface production (CLIP) [103], during which process cationic and free-radical polymerization are two significant types of polymerization. In essence, vat polymerization is the polymerization and crosslinking reaction initiated by UV light, rapidly forming long chains and cross-linked polymeric networks. In 1986, Charles Hull [90] invented the first 3D printer based on SLA and founded 3D Systems, making polymers the first materials to be applied in AM. The most highlighted features of SLA is its accurate resolution of 0.02 mm [104]. Lin *et al.* [86] used GO reinforced commercial polymer to fabricate the first 3D structure via SLA. Since then an increasing number of researchers have focused on

implementing GPMCs into SLA [105-108]. The issue on nozzle clogging in techniques like FDM can be averted as SLA is nozzle-free. SLA can also produce more than one product in one printing cycle. However, the disadvantage of photocurable materials prevents the large-scale development of SLA. A substrate support is greatly needed since the plastic is likely to incur deformation. Moreover, SLA equipment and good quality liquid resins are quite costly.

3.3. Material Extrusion

In the material extrusion based methods, materials are squeezed through a nozzle, where they are heated, then deposited and connected layer by layer. One commonly known material extrusion method is fused filament fabrication (FFF), also known as FDM [109] in which filaments are squeezed out of one or more extruders by heating thermoplastic materials. The molten polymers are deposited on a platform and fused together to form a 3D structure (**Fig.3c)**. FDM is widely investigated to fabricate ceramic, metal and polymer composites. So far, our literature search results indicate that only polymer matrices have been reported with regards to graphene-based composites via FDM. Wei *et al.* [110] first demonstrated graphene-based PLA and acrylonitrile butadiene styrene (ABS) composites with a GO loading up to 5.6 wt% via FDM. Numerous studies have focused on PLA/ABS as a matrix to fabricate GPMCs for a variety of applications such as electromagnetic shielding [111, 112], electrochemical sensing [113], energy storage devices [114] and tissue engineering scaffolds [115].

Direct ink writing (DIW) is another extrusion-based printing technique. Fluid materials like solutions, hydrogels, and pastes are extruded through nozzles by the force of a piston, a screw system, or by pneumatic pressure. The continuous filaments deposit on a platform and rapidly solidify, generating a 3D architecture. Rheological property (shear thinning behaviour) and a suitable viscosity (10^2–10^6 mPa·s, depending on the shear rate) of the printing ink for DIW is crucial and directly controls the final quality of the printing process [116]. The developed ink should possess shear thinning property, enabling smooth flow through the nozzle under shear stresses to achieve shape retention.

Research shows that high-aspect ratio graphene fillers can impart shear-thinning

behaviour. GO-containing ink has shown noteworthy printing capability and unique viscoelastic properties. Wang *et al.* [117] formulated water-based inks by functionalizing chemically modified graphene (CMG) with a responsive polymer (a branched copolymer surfactant, BCS). The interactions of the resulting ink can be regulated using the appropriate value of pH (**Fig.4a**). By modifying a GO reinforced resorcinol-formaldehyde (R-F) suspension, Zhu *et al.* [118] successfully fabricated lightweight, periodic graphene aerogel micro lattices via DIW (**Fig.4b-c**). The 3D printed graphene aerogels were lightweight, highly conductive and exhibited very high compressibility (up to 90% compressive strain). The resulting aerogels showed excellent mechanical property with an order of magnitude higher than bulk graphene materials in young's modulus. Based on previous studies, researches have focused on developing energy storage devices and sensors by GMPCs via DIW. Zhu *et al.* [119] utilized the above material to fabricate 3D-printed graphene composite aerogel microlattices for supercapacitors with exceptional capacitive retention (ca. 90% from 0.5 to 10 $A \cdot g^{-1}$) and power densities (>4 $kW \cdot kg^{-1}$) that equal or exceed those of reported devices made with electrodes 10−100 times thinner (**Fig.4d-g**).

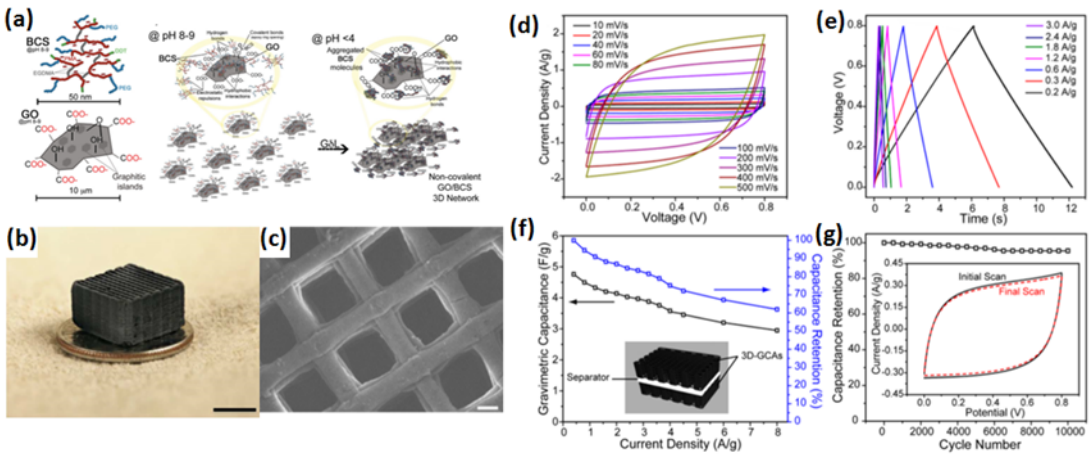

Fig. 4 (a) Simplified schematics depicting the proposed BCS and GO structures. Reprinted with permission from [117]. Copyright 2015 John Wiley and Sons. (b) optical image and (c) SEM image of a 3D printed graphene aerogel micro-lattice, Scale bars for (a) is 5 mm; (b) is 200 mm (b). Electrochemical performance of 3DGCA symmetric supercapacitor. Reprinted with permission from [118]. Copyright 2015 Springer Nature. (d) Cyclic voltammograms collected in 3 M KOH as a function of scan rate; (e) charge and discharge profiles collected at different current densities; (f) gravimetric

capacitance and capacitive retention calculated as a function of current density. Inset: a schematic illustration of the 3DGCA symmetric supercapacitor; (g) cycling stability tested at a scan rate of 200 mV/s for 10000 cycles. Reprinted with permission from [119]. Copyright 2016 American Chemical Society.

In order to form a suitable ink, the use of a suitable solvent is essential. However, the removal of this solvent may introduce porosity and defects into the matrix. Commonly, DIW is used to print polymer and ceramic with rapid solidification. A variety of polymer or hybrid polymer graphene-based composites have also been manufactured via DIW, including polycaprolactone (PCL)/graphene [120], polylactide-co-glycolide (PLG)/graphene [121], branched copolymer surfactant (BCS)/GO [117], poly(trimethylene carbonate) (PTMC)/graphene [122], polyurethane (PU)/GO [123], epoxy/graphene [124], which can be applied in Li-S batteries [125], biomedical smart nanomaterials [126] and gas sensors [85], etc. Furthermore, through synergistically leveraging the structural properties [127], biocompatibility [128], thermal and conductive properties of graphene-based materials [129], multifunctional ceramics can be effectively manufactured via DIW. Ladd *et al.* [130] reported that low viscosity liquid metal (such as alloys of gallium and indium) could be directly printed at room temperature. However, there is seldom report in relation to GMMCs via DIW methods.

3.4. Binder Jetting

Binder jetting, also known as 3DP, uses powder materials and an adhesive. This AM process prints a binder, which generally is in liquid form, into a powder bed and then fabricates layer by layer. Through a 3D computer model of the product, powdered materials are layered in a platform with an “ink-jet” printing technique used to bind the materials together (**Fig.3d**). 3DP has been used to prepare numerous materials, including ceramic, polymer and metal composites. The binder is one the key factor in the 3DP fabrication process [131]. However, the technique also presents challenges in terms of low printing resolution, surfaces roughness and low precision [132]. The weak binding between individual layers leading to weak and brittle objects is also limiting its further application. Therefore, there have been limited report about graphene-based composites via 3DP due to the low printing precision. Azhari *et al.* [133] firstly

reported electrodes using thermally rGO/palladium composite through a binder jetting method. The resulting thick supercapacitor electrodes with porous microstructure demonstrated high gravimetric and areal capacitance values of 260 F g^{-1} and 700 mF cm^{-2}, respectively.

4. Graphene-based Composites via AM

Owing to the unique properties of graphene, numerous researches have focused on developing composites with graphene related materials as a dispersed nanofiller in various matrices, including ceramics [38, 134], metals [135-137] and polymers [132, 138, 139]. A large majority of these efforts focus on how to homogeneously disperse graphene nanofillers in these matrices. In the case of polymer composites the exceptional properties of graphene do not readily transfer into exceptional composite properties (e.g., high strength, thermal and electrical conductivity) due to issues related to filler dispersion. Similarly, also the development of graphene-modified metals or ceramics is hindered by inhomogeneous dispersion of graphene into these matrices and the necessity of high temperature and pressure processing.

4.1. Graphene-based Ceramic Matrix Composites

Ceramics are broadly used in biomedical, electronic, automotive, industrial and space applications because of their high stiffness, strength, and stability at high temperatures [140, 141]. However, properties like embrittlement and low electrical conductivity prevent traditional ceramics from wider applications. Graphene can fairly compensate the drawbacks of ceramics. The development of GCMCs via AM is still in its infancy. Currently, some ceramic matrices (calcium phosphate, aluminium oxide, aluminium carbide and polymer derived ceramics) have been successfully fabricated using graphene related materials as an additive via AM [93, 127, 129, 142], and will be described below in more detail.

4.1.1. Aluminium Oxide (Al_2O_3)/Graphene

Al_2O_3, like other ceramics, owns properties like high compressive strength, high temperature resistance, chemical and corrosion resistance. Particularly, Al_2O_3 is

widely used as a structural ceramic material at high temperatures. Conversely, like other ceramics, low fracture toughness and thermal shock resistance of Al_2O_3, as well as decreasing fatigue strength at high temperatures, restrict its applications. To solve this issue, researchers have focused on the fabrication of graphene reinforced Al_2O_3 composites [31-33]. However, studies on graphene reinforced Al_2O_3 composites fabricated using AM techniques are few, and only one paper was retrieved. Tubío *et al.* [127] firstly confirmed the printability of GO/Al_2O_3 composite with well-defined complex mesoscale architecture via a DIW method by basic rheological and morphological studies.

4.1.2. Calcium Phosphate (CaP)/Graphene

This refers to a kind of ceramic material consisting of calcium ions (Ca^{2+}) and phosphate ions (metaphosphates-PO^{3-}, orthophosphates-PO_4^{3-}, and pyrophosphates-$P_2O_7^{4-}$). CaP is usually used as a biomaterial because it has a composition resemblance to bone and teeth. Ca to P ratio is a decisive factor which significantly determines the dissolution and bioactivity performance of different CaPs. A low Ca to P ratio provides an acidic environment leading to an improvement in the dissolution rate of CaPs. Among all the CaPs, hydroxyapatite (HA, $Ca_{10}(PO_4)_6(OH)_2$) has great bioactivity with a Ca to P ratio of 1.67 to 1, which is similar to the composition of natural teeth and bone. Tricalcium phosphate (TCP, Ca:P = 1.5:1) has a somewhat lower bioactivity compared to HA. To fully leverage biocompatibility properties of graphene-based materials, CaP in combination with graphene has been studied for biomedical applications. Wu *et al.* [142] reported a GO modified β-tricalcium phosphate (β-TCP-GRA) scaffold by producing a 3D printed β-TCP scaffold and then soaking it in a GO/water suspension in combination with a heat treatment (**Fig.5a**). Compared to a scaffold without GO modification, the β-TCP-GRA scaffold showed enhanced biological properties (the cell proliferation, alkaline phosphatase activity and osteogenic gene expression) with human bone marrow stromal cells (hBMSCs). Zhang *et al.* [143] adopted a similar strategy to produce a Fe_3O_4 nanoparticles/GO nanocomposite modified β-TCP scaffold (β-TCP–Fe–GO). The resulting β-TCP-Fe-GO was magnetic as well as possessed osteogenic capabilities, which was promising in bone tumour therapy. Both TCP scaffolds were printed via a DIW method and subsequently soaked in a GO or GO-Fe

suspension. GO was coated on the surface of the scaffolds without having to consider the problem of dispersing GO in the matrix. Jakus *et al.* [128] investigated a hybrid material (HA:graphene = 1:1 v/v) exhibiting not only good bioactivity but also 3D-printability, electrical conductivity ("conductivity gap" of nearly 450 S/m over a graphene compositional range from 35 to 40 vol%) and flexibility. In vitro experiments of hyperplastic bone (HB)-3D-graphene (3DG) using mesenchymal stem cells showed that this hybrid material performed well in terms of cell viability and proliferation (**Fig.5b**).

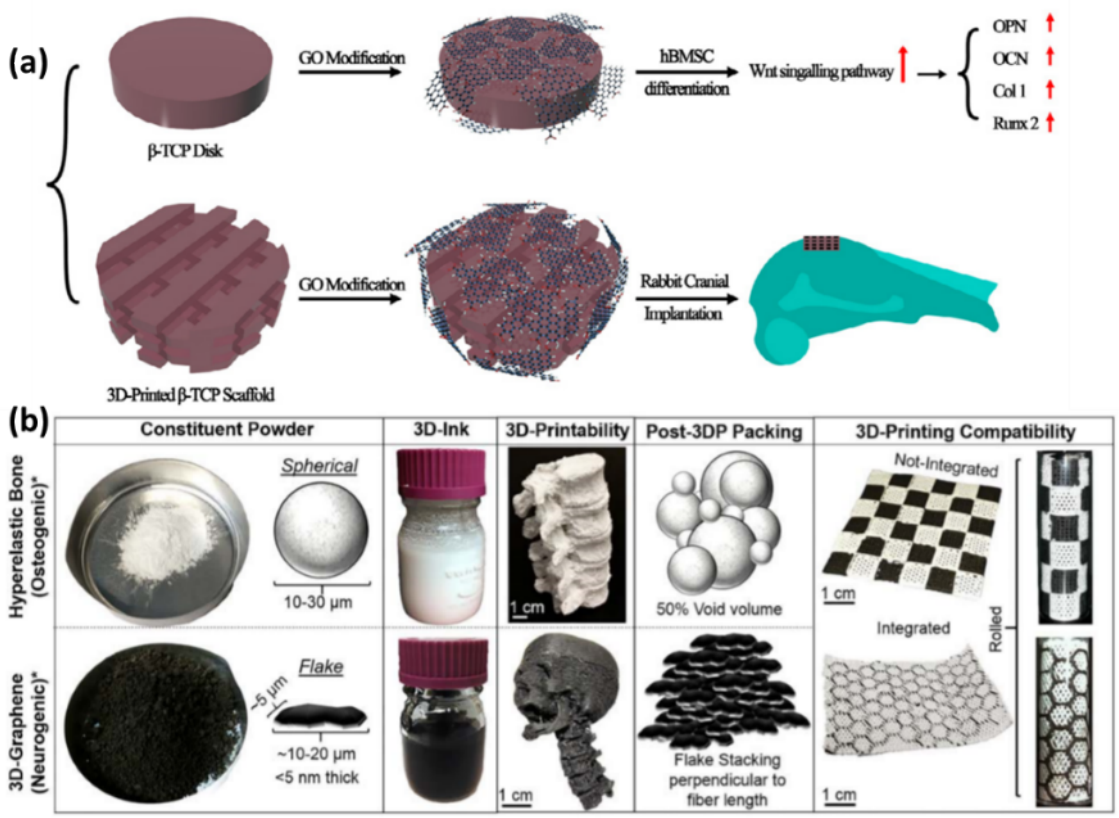

Fig. 5 Scheme illustration of (a) GO modification β-TCP bioceramic stimulates the in vitro and in vivo osteogenesis. Reprinted with permission from [142]. Copyright 2015 Elsevier. (b) HB and 3DG ink systems, their powder constituents, resulting 3D-inks, and 3D-printability. Reprinted with permission from [128]. Copyright 2017 John Wiley and Sons.

4.1.3. Polymer Derived Ceramics/Graphene

Polymer derived ceramics, known as preceramic polymers, are ceramic materials that are based on a polymeric phase and are produced from the transformation of

polymeric precursors, like silicone resins and geopolymers [144]. Tailored composition and microstructure of polymer derived ceramics can be predesigned by varying the formula of precursors and the conversion of ceramics can occur at a relatively low temperature [145]. Before polymer derived ceramics are transformed into ceramics, some properties, like rheological behaviour, resemble that of a polymer, which means that polymer derived ceramics are easier to shape into complex structures or architectures. What's more, nanofillers can be dispersed in preceramic polymers in a simpler and more efficient manner than in ceramics. A GO/SiOC ceramic scaffold was fabricated by Pierin *et al.* [146] by using a preceramic silicone polymer ink. The addition of 0.1 wt.% GO immensely improved the compressive strength of the SiOC scaffold from 2.5 to 3.1 MPa. Zhong *et al.* [129] produced GO/geopolymer (GOGP) composites via an extrusion method. A thick layer of water film formed between the GO and aluminosilicates particles, well explaining the effect of GO on the rheology of GOGP (**Fig.6**).

The majority of the introduced GCMCs are manufactured via DIW. During the DIW process, ceramic paste with graphene related materials is extruded from a nozzle. Typically, the 3D printed objects are sintered in order to obtain good mechanical strength. DIW method requires relatively little energy, but its accuracy is quite low. As the solvent and other additives evaporate or decompose after sintering, the structures can be distorted.

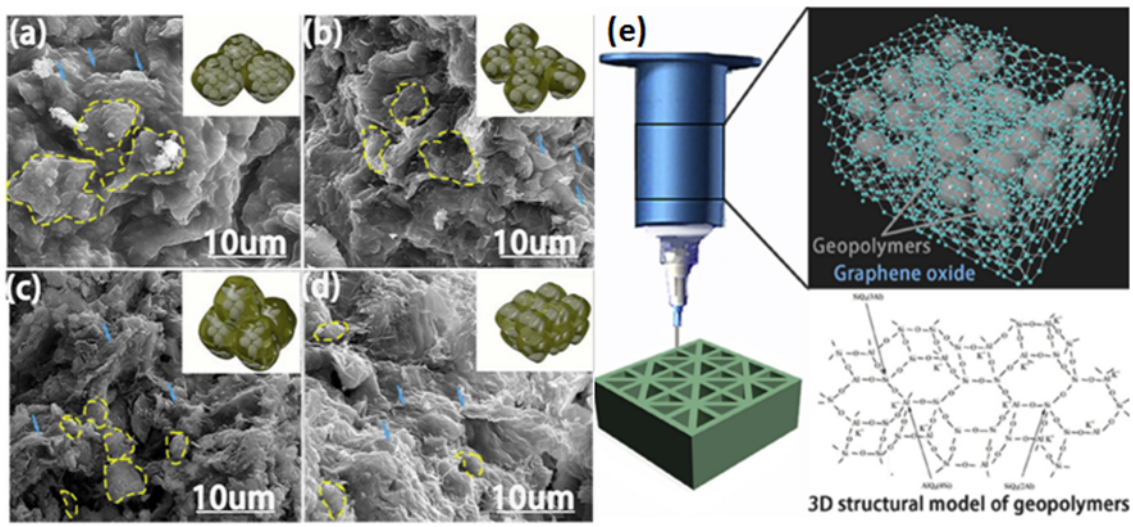

Fig. 6 (a-d) SEM images and corresponding models illustrating the HPPG encapsulation

by GO layers. As the loading of GO in the nanocomposite increased, the size of the particle agglomerates (marked by dotted-line circles) that are encapsulated within the GO films decreases; (e) illustration of the 3D printing process with the chemical structure of the geopolymer. Reprinted with permission from [129]. Copyright 2017 Elsevier.

4.1.4. Calcium Silicate ($CaSiO_3$)/Graphene

$CaSiO_3$ is considered to be a potential biomaterial, but its poor mechanical properties limit further applications in the biomedical field [147-149]. Shuai *et al.* [46] fabricated a $CaSiO_3$/graphene(0.5 wt.%) composite scaffold via SLS with improvement by 46% and 142% in the fracture toughness and compressive strength, respectively. Particularly with ceramics with a very high melting point and in comparison with other sintering methods, SLS is a very appealing processing technique as it can limit the thermal effect of high sintering temperature on graphene, by reducing the sintering time to seconds or milliseconds [46].

4.2. Graphene-based Metal Matrix Composites

Recently, the demands for metal matrix composites (MMCs) have increased rapidly as the mechanical strength, thermal conductivity and electrical conductivity of MMCs are outperforming many other matrix materials. In order to further enhance the multifunctional properties of MMCs, numerous researches have tried to use graphene related materials as a nanofiller to modify metal matrices [137, 150, 151]. However, there are only few reports on AM graphene-based MMCs, except for some researches using laser-based powder bed fusions. Lin *et al.* [61] added single-layer GO into an iron matrix through a laser sintering AM method. Meanwhile, laser irradiation melted the iron powders into liquid and the fast laser heating and cooling process prevented aggregation of GO powders (**Fig.7a-b**). The mechanical performance and fatigue life of laser sintered GO (2 wt.%)/Fe composite were improved significantly, with the fatigue life being 167% higher than that of the laser-sintered pure Fe reference sample. Since unsatisfactory microstructures and accumulated residual stresses may form during the high temperature laser processing, the mechanical performance of laser

sintered AM components will be limited. Lin *et al.* [152] proposed a hybrid manufacturing process combining laser shock peening and laser sintering of GMMCs. A strengthened metal/graphene interface was formed as shock waves pass through and bounce back between graphene sheets, leading to a good resistance to fatigue of the GMMCs (**Fig.7c**).

Wang *et al.* [153] firstly reported a GNP reinforced nickel-based superalloy (Inconel 718, a Ni–Cr–Fe austenitic superalloy). Tensile strength and Young's modulus of the 1.0 wt.% graphene-reinforced Ni composites were enhanced by 51% and 42%, respectively. Load transfer, thermal expansion coefficient mismatch, and dislocation hindering were three important mechanisms for main contribution to the reinforcement of the composites.

Hu *et al.* [94, 95] fabricated graphene reinforced aluminium and copper GMMCs via SLM and obtained an 18% improvement in average modulus (119 GPa) of the graphene reinforced copper. The Vickers hardness achieved 75% and 50% improvements compared to that of pure aluminium and copper, respectively. An Al_4C_3 phase was observed through the XRD and HRTEM data. The realization of Al_4C_3 nanorods was attributed to the relatively low free energy of formation (-196 kJ/mol at 298 K) [154] of Al alloys and carbon (graphite, carbon fibres, CNTs, or graphene). Zhou *et al.* [93] introduced an Al_4C_3/Al composite through an *in-situ* inter-reaction between GO and aluminium alloys. The mentioned GMMCs are fabricated via a laser-based method with relatively high accuracy. But this process consumes large amounts of energy because of the high melting point of most metallic materials. Additional manual/automatic mechanical or electrochemical polishing is required to alleviate the surface roughness of 3D printed objects. Besides, a metal SLS 3D printer is expensive (≥ 300,000 US dollars).

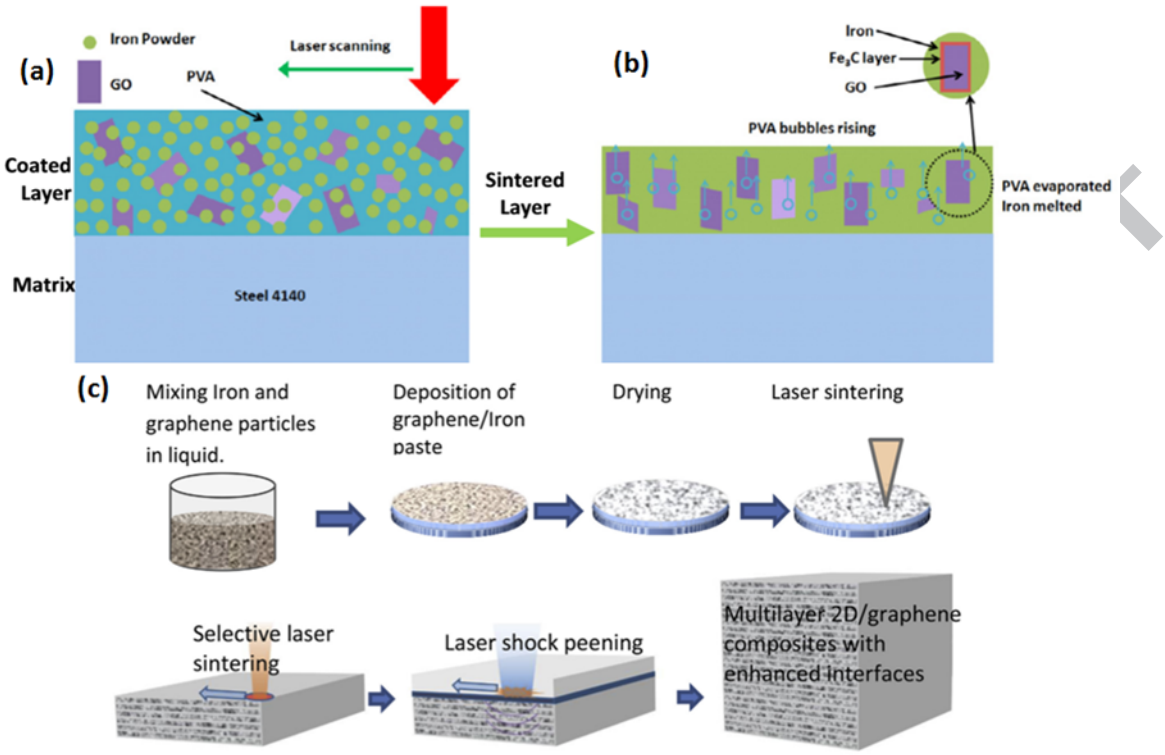

Fig. 7 Schematic of laser deposition of a GO/Fe nanocomposite layer (a) after coating and (b) after laser sintering. Reprinted with permission from [61]. Copyright 2014 Elsevier. (c) layered laser sintering process with shock loading to control the graphene/metal interfacial microstructures. Reprinted with permission from [152]. Copyright 2018 Elsevier.

4.3. Graphene-based Polymer Matrix Composites

Polymers are suitable for the majority of AM technologies owing also to relatively low processing temperature compared to ceramic or metal matrices. A wide range of thermoplastic and thermoset polymers can be processed via AM, for instance PLA [155], PCL [156], ABS [110], PVA [157], polycarbonate urethane (PCU) [158], epoxy [124] and photosensitive resin [107]. Nanofillers like graphene and its derivatives are introduced into polymers to create high-performance nanocomposites with a high strength-to-weight ratio and additional multifunctional properties [159]. However, several problems still exist in the processing of graphene-based polymers via AM. Firstly, according to most studies, it is essential to form a homogeneous dispersion of the graphene nanofillers in the polymer matrix to obtain optimal properties, with each dispersion technique (e.g., ultrasonication [160], three roll milling [161, 162], high

shear mixing [163], simple mechanical mixing [164], ball milling [165] and hot pressing [166], etc.) having its own limitations and deficiencies. Currently, a common issue is the phase separation between polymers and graphene sheets occurring during the synthetic process. In addition, aggregation of graphene sheets can clog the nozzle of the printer, resulting in breakdown of the printing process. This section will give a detailed discussion of the polymer matrix materials used to fabricate graphene-based polymer matrix composites (GPMCs) via four specific AM methods (SLS, SLA, DIW, and FDM).

4.3.1. Graphene-based Thermoplastic Polymer Composites

Through melting and subsequently cooling layer by layer, thermoplastic polymers can be processed by various AM methods. The most frequently used thermoplastic polymers are ABS, polyamide (PA), PMMA, as well as some biocompatible polymers such as PLA, PCL and PVA. Numerous studies seek to introduce graphene to address the low stiffness and strength of the thermoplastic resin. Below we will give a brief overview of graphene-based thermoplastic polymers recently reported.

ABS/graphene nanocomposites

Researches [167, 168] have implemented FDM to fabricate ABS/graphene composites which showed an improvement in elastic modulus, thermal conductivity and electrical conductivity, compared with pure ABS materials. Wei *et al.* [110] were the first to print graphene-related materials via FDM directly using ABS. However, a deterioration in tensile strength was observed which may be caused by local stresses concentrations generated by GNPs or agglomerated GNPs.

PA/graphene nanocomposites

De Leon *et al.* [97] developed a rGO-coated PA composite which established a fine conductive network of nanoparticles, thereby resulting in a lower percolation threshold than traditional approaches like solution or melt compounding methods. SLS was used for the manufacturing of the first metal-free electrostatic motor based on fully 3D printed parts based on rGO-coated PA material.

PBT/graphene nanocomposites

Gnanasekaran *et al.* [169] chose polybutylene terephthalate (PBT) as a matrix for hybrid nanofillers (carbon nanotubes and graphene) to fabricate an FDM-based conductive nanocomposite. Multiple printing heads were used in this process which could fabricate far more than one material at once to manufacture functional structures and properties (e.g., elastic behaviour and conductive properties) at low cost.

PMMA/graphene nanocomposites

Mohan *et al.* [170] produced super high electrical conductive hybrid polymer-graphene composites (electrical conductivity of 14.2 S/cm, please refer to **Table 3** for more comparison) via FDM used solvent cast polymethyl methacrylate (PMMA)-based filament with 10 wt.% polypyrrole and 10 wt.% graphene.

PLG/graphene nanocomposites

Jakus *et al.* [121] developed 3D printable inks consisting of polylactide-co-glycolide (PLG) and a high concentration of graphene (60 vol.% of solid). The resulting 3DG material had a high electrical conductivity of 800 S/m and excellent functional properties (e.g., biocompatibility, mechanically flexible, neurogenically bioactive, biodegradable, and surgically friendly), confirming that 3DG materials show great promise in many applications, such as, wearable and implantable electronics, sensors, and tissue engineering, etc. (**Fig.8a-e**).

PVB/graphene nanocomposites

Huang *et al.* [84] prepared a printable ink by adding a high concentration of GNPs into polyvinyl butyral (PVB). The shear stress in the nozzles resulted in GNP alignment in the axial direction, resulting in electrical anisotropy (**Fig.8f-h**).

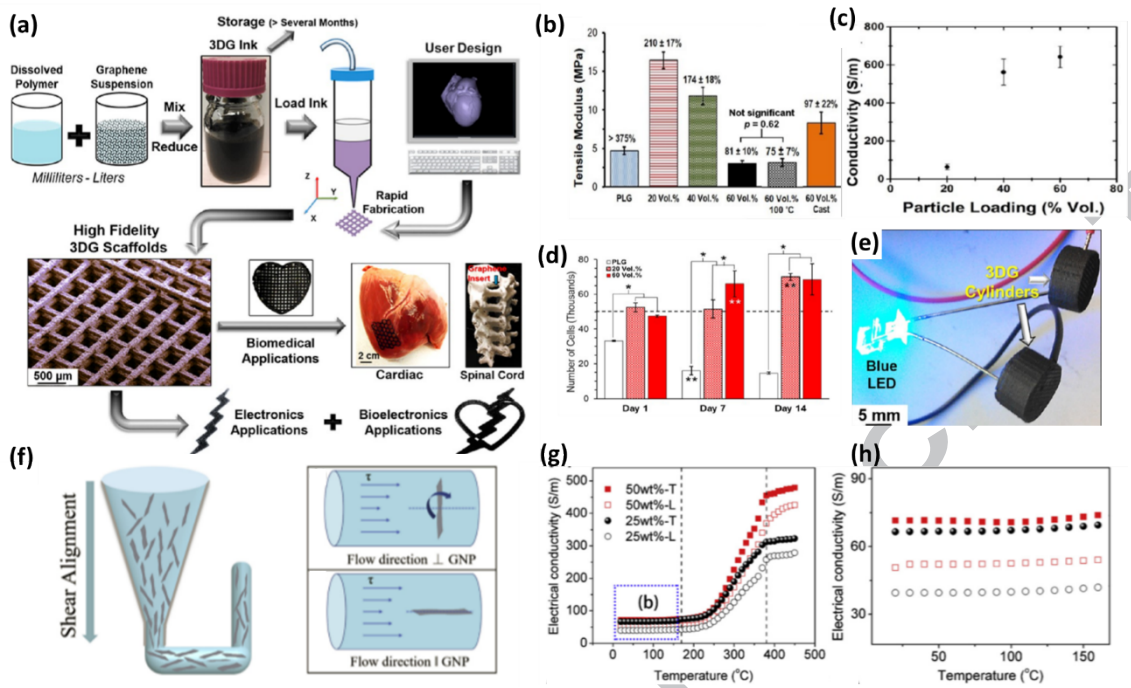

Fig. 8 (a) 3DG inks are produced through a simple combination and mixing an elastomeric solution with a dispersion of graphene powder in a graded solvent followed by volume reduction and thickening, a process that can be scaled up to many litres at once if desired. User-defined architectures 3D-printed from 3DG have a variety of potential applications, including those relating to energy storage and bioelectronics, as well as tissue and organ engineering; (b) corresponding elastic moduli obtained from tensile tests and average percent strain-to-failure; (c) conductivity of non-annealed fibre extruded from a 400 µm diameter tip; (d) number of hMSCs present on the scaffolds; (e) demonstration of electrical conductivity of objects as-printed, showing two 3DG cylinders incorporated into a circuit with a blue LED. Reprinted with permission from [121]. Copyright 2015 American Chemical Society. (f) Schematic of shear alignment; (g) electrical conductivity versus temperature for 25 wt.% and 50 wt.% 3D graphene scaffolds; (h) zoom-in region between RT and 170 ℃. Reprinted with permission from [84]. Copyright 2018 Elsevier.

PCL/graphene nanocomposites

Sayyar *et al.* [120] were the first to use extrusion-based techniques to fabricate a polycaprolactone (PCL)/graphene scaffold with 143% and 50% increase in Young's modulus and tensile strength and great improvement in biological property. Wang *et*

al. [156] found that surface treatment of sodium hydroxide (NaOH) on PCL/pristine graphene scaffolds by DIW can make the scaffolds hydrophilic without influencing their biocompatibility.

PVA/graphene nanocomposites

Shuai *et al.* [96] fabricated a porous GO (2.5 wt.%)/PVA nanocomposite scaffold via SLS with 60%, 152% and 69% improvement in compressive strength, Young's modulus, and tensile strength, respectively (Please refer to a summary of mechanical properties in **Fig.13**). Cell culture studies of human osteoblast-like MG-63 cells were grown and proliferated well on the GO/PVA scaffold indicating good cytocompatibility of the GO/PVA scaffold (**Fig.9**).

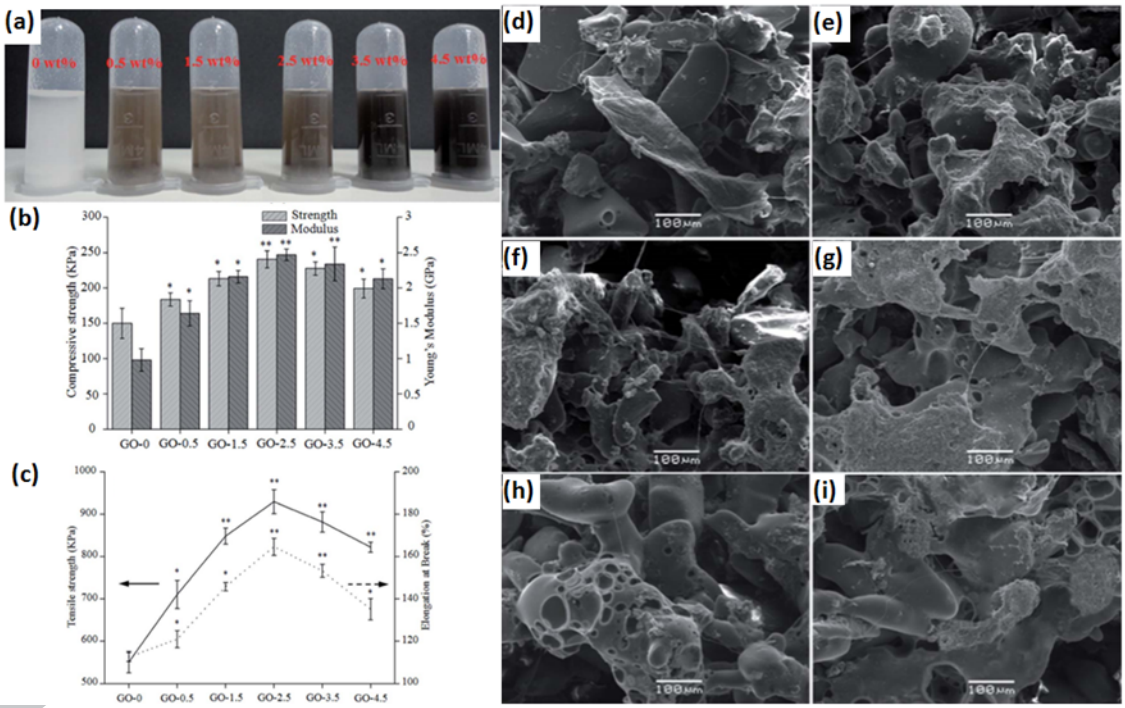

Fig. 9 (a) Images of GO/PVA suspensions with various GO loadings; (b) compressive strength and Young's modulus of GO-0, 0.5, 1.5, 2.5, 3.5 and GO-4.5; (c) tensile strength (solid line, left axis) and elongation at break (dotted line, right axis) of GO-0, 0.5, 1.5, 2.5, 3.5 and GO-4.5; (d-g) SEM images of the MG-63 cells attaching and spreading on the surfaces of GO-2.5 scaffolds and (h-i) GO-0 scaffolds after (d) 1 day; (e and h) 3 days; (f) 5 days and (g and i) 7 days of incubation. Reprinted with permission from [96]. Copyright 2011 Royal Society of Chemistry.

PLA/graphene nanocomposites

Vernardou *et al.* [111] prepared PLA/graphene conductive polymer composites via FDM with good electrochemical behaviour (discharge capacity of 265 mAh/g with retention of 93% after 1000 cycles, please refer to **Table 4** for more details). A graphene-based PLA composite was also studied by Foster *et al.* [114], the FDM printed material was applied as freestanding lithium-ion anodes and solid-state graphene supercapacitors (**Fig.10**). Despite the output was far from the current state-of-the-art performances, this kind of supercapacitor (consisting of 8 wt.% graphene and 92 wt.% PLA) still worked as a battery material. Chen *et al.* [28] added GO into TPU with PLA via a solvent mixing process and manufactured a scaffold by FDM. It was found that GO not only significantly enhanced the mechanical properties but also was beneficial to cell proliferation.

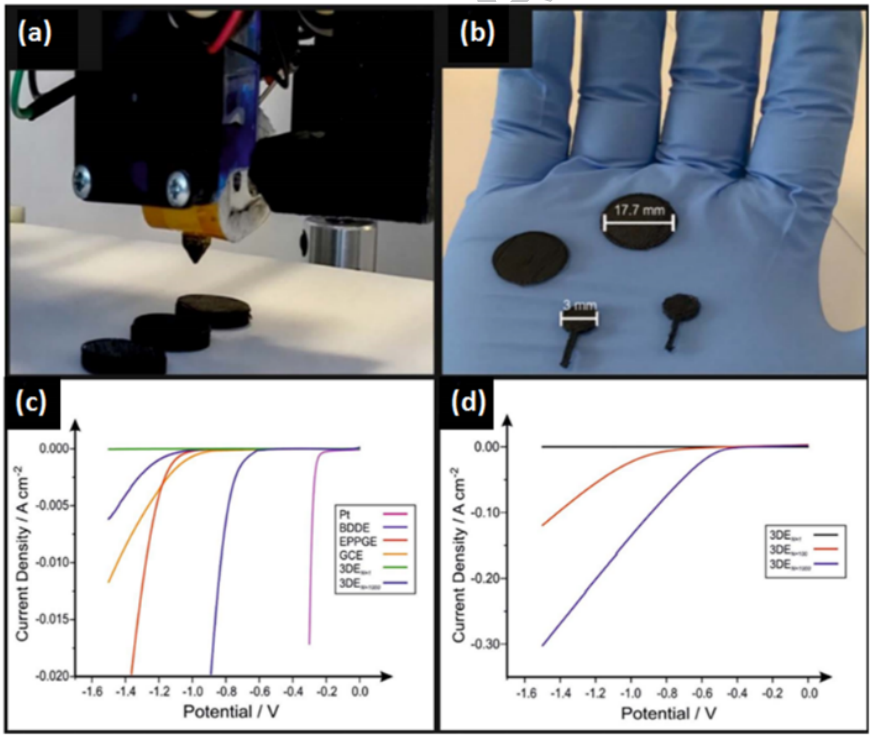

Fig. 10 (a) The 3D printing process and (b) a variety of printed 3DEs used in Foster et al. Comparative linear sweep voltammograms (c) using 3DE compared to EPPGE, GCE, BDDE and platinum show the onset of the hydrogen evolution reaction. Stability studies of the 3DEs (d) using linear sweep voltammograms for the initial, 10th, 100th and 1000th scans. Reprinted with permission from [114]. Copyright 2017 Springer Nature.

4.3.2. Graphene-based Thermosetting Polymer Composites

Thermosetting resins undergo an irreversible crosslinking reaction which polymerises monomers into insoluble polymers by heat or other conditions (e.g., light). Thermosetting polymers possess advantages such as high stiffness, strength and thermostability while they are too fragile. The introduction of graphene sheets may alleviate the brittleness of thermosetting polymers. Development of graphene-based thermosetting resins via AM method is believed to have great potential for creating new materials that enable 3D printing of multifunctional components.

Epoxy/graphene nanocomposites

Compton *et al.* [124] printed epoxy/graphene composites via DIW method, and compared with cast neat epoxy the developed epoxy/graphene composites were 67% stiffer, and possessed low bulk resistivity. It is promising in the field of packaging of sensitive electronic components for its electrostatic discharge properties and applications requires electromagnetic shielding properties.

Graphene-based photopolymer resins

Activated by UV light, photopolymer resins can polymerise during the process of vat photopolymerization based 3D printing technologies. The thermomechanical properties of photopolymers can be improved by the introduction of graphene fillers. However, limited research [171-173] implemented SLA to produce graphene-based polymer composites because of the deterioration in printability and mechanical properties when graphene is introduced. Moreover, the presence of graphene can block the UV light during the SLA process and interfere with the photocuring process of the resin. Wang *et al.* [171] recommended a graphene content less than 5 wt% to maintain the appearance and mechanical strength of the printed object.

Owing to the functional groups attached to GO, strong interfacial bonds are well formed between GO nanofillers and polymer matrices. Lin *et al.* [86] used GO reinforced commercial polymers (model Pic 100 from EnvisionTEC) to fabricate the first 3D structure via SLA. The tensile strength and elongation were increased by 62% and 13% with the addition of 0.2 wt.% GO, respectively. Korhonen *et al.* [105] printed

a GO/acrylic resin structure via SLA. Under nitrogen atmosphere, the samples were pyrolyzed to reduce GO and to eliminate the polymer, obtaining rGO flakes with good electrical conductivity (**Fig.11a-b**). Manapat *et al.* [107] made use of the metastable, temperature-dependent characteristic of GO to improve the mechanical properties of 3D-printed commercial resin by SLA. After thermal annealing at 100 °C for 12 h, an enhancement in tensile strength of 674% with 1 wt.% GO loading was obtained (**Fig.11c-f**)

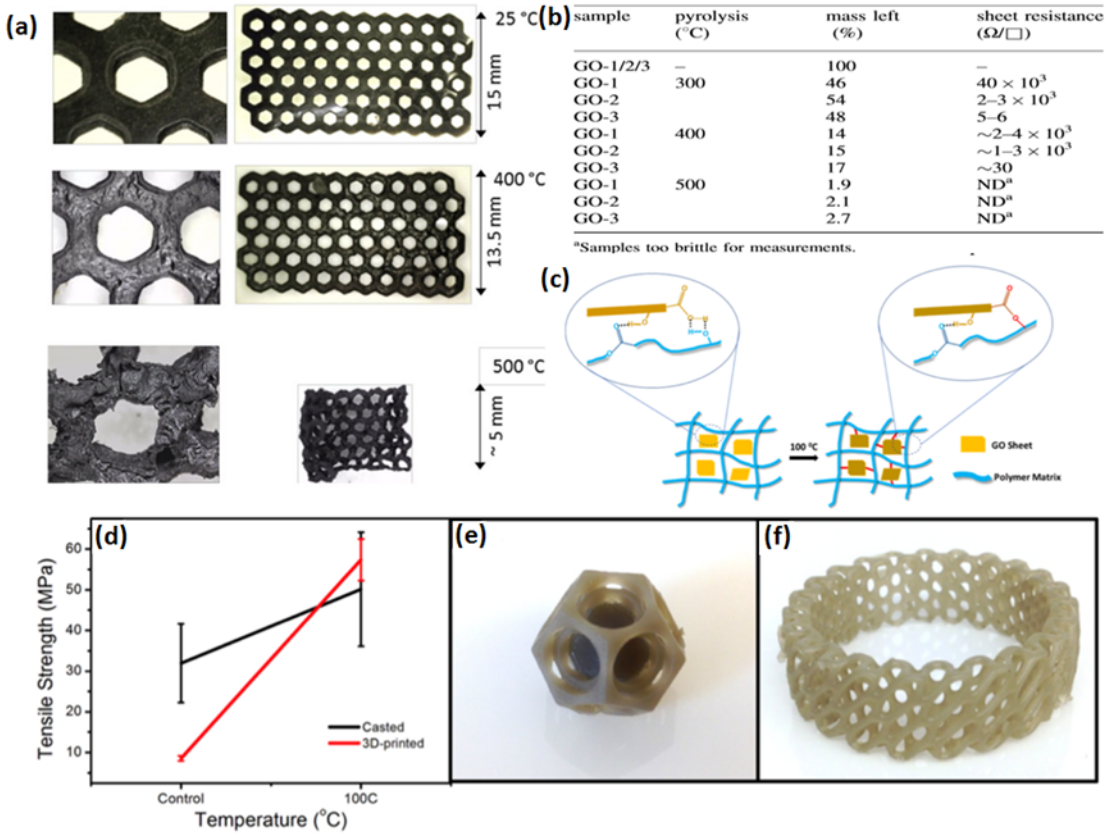

Fig. 11 (a) Photographs and microscopy images and (b) electrical properties of samples after different pyrolysis steps. Reprinted with permission from [105]. Copyright 2015 John Wiley and Sons. (c) Schematic diagram of proposed covalent and non-covalent interaction of 3D-printed GO nanocomposites; (d) tensile strength comparison of the cast and 3D-printed parts. SLA-printed complex-shaped GO nanocomposites: (e) nested dodecahedron and (f) diagrid ring. Reprinted with permission from [107]. Copyright 2017 American Chemical Society.

Gelatin methacrylate-poly(ethylene glycol) diacrylate/GO (GelMA-PEGDA/GO) scaffolds with hierarchical structures via SLA were developed by Zhou *et al.* [108]. It

was found that GO-induced chondrogenic differentiation of human mesenchymal stem cells (hMSCs), resulting in the promotion of glycosaminoglycan and collagen levels. A GelMA-PEGDA scaffold incorporated with 0.1 mg/ml GO was found to have the highest proliferation with an increase of 22% compared to that of the reference sample (**Fig.12a-d**). A projection micro SLA technique was utilized to fabricate arbitrary complex hierarchical 3D micro architected graphene foams (with 3D spatial features sizes of ~10 µm and pore sizes of ~60 nm) (**Fig.12e-l)** [174], alleviating the problem of the poor mechanical properties and showing enhanced mechanical properties (100 MPa) at low density of 0.2 g/cm^3, which is highly desirable for electrode materials that can experience severe mechanical stress during energy storage cycling.

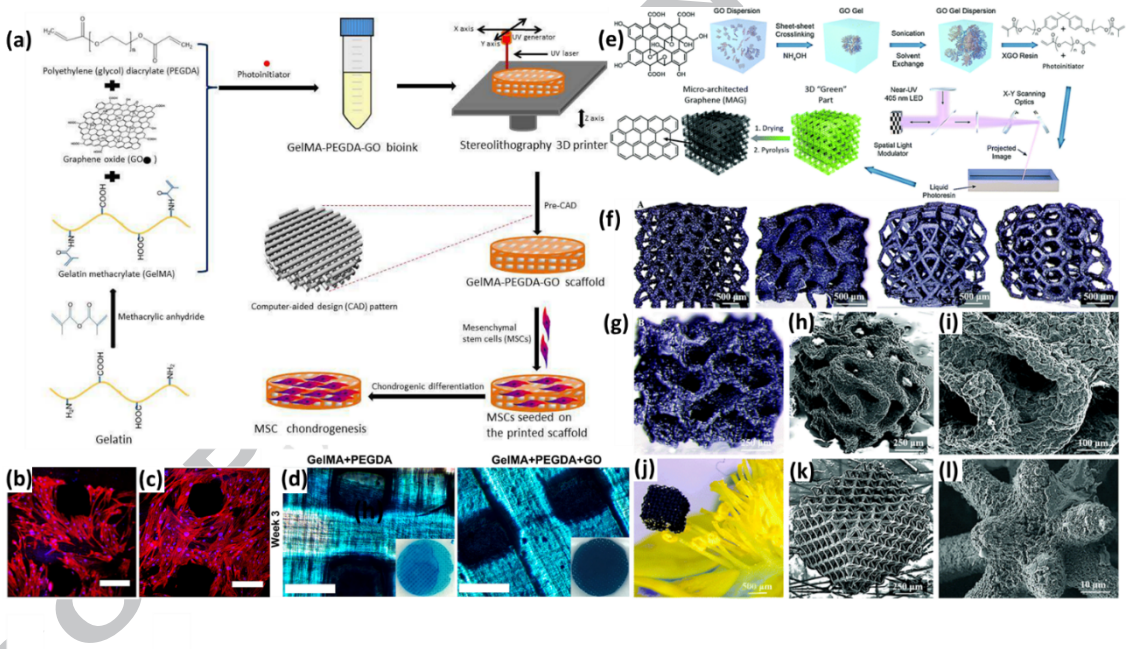

Fig. 12 (a) Schematic diagram of 3D printed GO scaffold for promoting chondrogenic differentiation of hMSCs. Confocal micrographs of 5-day MSC proliferation on GelMA-PEGDA scaffolds incorporated with (b) 0 mg/mL; (c) 0.10 mg/mL concentrations of GO. Scale bar = 200 mm. The cytoskeleton and cell nuclei were stained by Texas Red®-X phalloidin (red) and DAPI (Blue). (h) Alcian Blue stained micrographs of mesenchymal stem cells (MSCs) after chondrogenic differentiation on the surface of the GelMA-PEGDA scaffolds without and with GO over 3 weeks. Scale bar = 200 mm. Reprinted with permission from [108]. Copyright 2017 Elsevier. (e) Scheme of resin synthesis and processes to achieve micro-architected graphene (MAG). (f) Four "Green" MAG parts

of differing unit-cell structures before pyrolysis; (g) optical and (h-i) SEM image of pyrolyzed gyroid; (j) optical and (k-l) SEM image of pyrolyzed MAG octet-truss. Reprinted with permission from [174]. Copyright 2018 Royal Society of Chemistry.

5. Properties and Applications of GPMCs

Although there are many challenges with respect to shape preservation, printing accuracy, low mechanical strength and types of materials in developing GPMCs for 3D printing, these materials have been studied for a range of applications including biomedicine, electronics, sensors, electromagnetic shielding, etc. This section overviews some of the most promising perspective applications.

5.1. Mechanical Properties and Strain Sensor Application

Recently, Gao *et al.* [175] utilized a highly cost-effective strategy, multilayer coextrusion technique to fabricate a multilayer composite structure of alternating layers of neat PLA and PLA containing 1 wt.% GNP with 120% reinforcement in tensile modulus, which was attributed to the high degree of planar alignment, improved dispersion and relative large aspect ratio of GNPs after multilayer coextrusion. The possibility of creating both structural and functional systems is even more feasible for graphene filled nanocomposites due to its larger specific surface area, great interfacial interaction, and outstanding properties [176]. Compared to conventional processing methods, AM methods may offer GPMCs better mechanical property enhancements as the layer-by-layer fabrication method can align the nanoplatelets. Feng *et al.* [177] fabricated 0.5 wt.% graphene reinforced PU resin using a DLP method. In this case, the flexural modulus and fracture toughness were improved by 14 % and 28 %, respectively, compared to the neat resin.

Surface modification of graphene nanoparticles can improve the compatibility of the nanofiller with the polymer matrix via the formation of covalent bonds, resulting in the effective improvement of mechanical properties. Li *et al.* [106] functionalized GO with 2-hydroxyethyl methacrylate (HEMA-g-GO) before dispersing it in a acrylate photosensitive resin, to prepare nanocomposites by SLA. The results suggested that the tensile strength and flexural strength of nanocomposites were increased by 67%

and 32%, respectively, by adding only 0.06 wt.% of HEMA-g-GO. As a comparison, **Fig.13** compiles the improvement in Young's modulus and tensile strength of several materials via different AM methods.

Huang *et al.* [178] incorporated graphene into polydimethylsiloxane (PDMS) to a produce tunable and highly sensitive strain sensors via DIW with a large gauge factor (up to 448 at 30% strain) and durability (100 compress-release cycles under 10% strain).

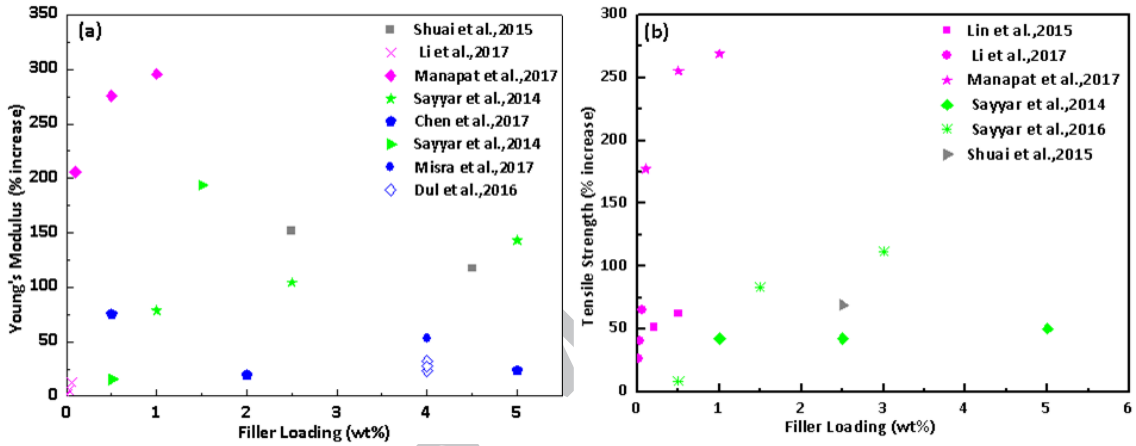

Fig. 13 A summary of (a) Young's modulus (% increase) and (b) tensile strength (% increase) as a function of graphene filler loading of polymer nanocomposites via different AM methods from the literature. Purple represents SLA, green represents DIW, blue represents FDM, and gray represents SLS [28, 86, 96, 106, 107, 115, 120, 122, 167].

5.2. Electrical Conductivity and Applications

The intrinsic conductivity of graphene depends on both the synthesis method and surface modification [179]. In particular, the intrinsic conductivity of graphene depends on the number of defects (reactive sites) that can be found on the surface. These defects are usually generated during the oxidation-reduction process of GO [62, 180]. These processes yield rGO with variable carbon-oxygen ratios generating discontinuities on the electronic delocalization of filler and consequently, reducing its conductivity by orders of magnitude. Reduction favours sheet crystallization and the formation of graphitic structures. In order to avoid restacking or agglomeration of the layers, grafting molecules such as hexylamine [181], or phenyl isocyanate [176, 182] are commonly used on the surface of graphene. However, this chemical grafting

generates surface defects in the sheets that again reduce their electrical properties.

At very low filler loading, electrical properties are dominated by the dielectric matrix so the composite is essentially non-conductive. As the graphene content increases, the dielectric distance that separates the sheets decreases. Above the percolation threshold, continuous conduction paths are created within the polymer matrix and the electrical conductivity suddenly increases [183]. Nevertheless, sheet-sheet junctions are highly resistive (for nanotubes, the contact resistance is in the order of 1 MΩ) [184], and it has been proposed that the main conduction mechanism is tunnelling [185, 186].

Current researches on graphene surface engineering to prepare conductive composites is focusing on the following, often contrasting, challenges: a) to generate minimum defects within the graphene sheets, b) to improve the graphene compatibility with polymer matrices (good dispersion, good reinforcement and lower percolation threshold), c) to impart resistance to the chemical or electrochemical reduction; d) to reduce the sheet-sheet junction resistivity in order to obtain a good conductive network for electronic transport [179] and e) to obtain larger aspect ratio particles [162, 187]. The electrical properties of graphene-modified polymer nanocomposites, prepared by AM, are summarized in **Table 3** below.

Graphene, has been extensively studied in energy storage devices and electrochemical sensors. The applications of GPMCs in electronic devices are mainly divided into two aspects, one is as a potential material in electrochemical energy storage devices, and the other is electronic sensors with great versatility and reduced prices. Fu *et al.* [188] selected lithium iron phosphate (LFP) and lithium titanium oxide (LTO) as cathode and anode materials, used in combination with GO, to generate printable inks and fabricate electrodes by DIW process. Then, a polymeric material was used to fill the channel between the cathode and anode. The printed cathode and anode demonstrated good cycling stability. **Table 4** summarizes the use of GPMCs produced by AM in energy storage.

Owing to their high specific surface area, chemical stability, excellent electrical properties and low temperature catalytic performance, graphene related materials

are a great candidate material for humidity sensors [189], electrochemical sensors [190], gas sensors [150] and biosensors [191]. The conventional methods to fabricate graphene-based sensor devices involve multiple chemical steps. The advantage of AM is to provide a simpler and more convenient way to fabricate these devices.

Table 3 The electrical properties of GPMCs via different AM methods

AM method	Matrix	Filler	Electronic properties	Refs
DIW	PLG	75 wt.% graphene	~ 875 S/m	[121]
	BCS	3 wt.% GO	40 S/m	[117]
	R-F	20 mg/ml GO	87 S/m	[118]
		40 mg/ml GO	198 S/m	
		40 mg/ml GO	278 S/m	
	Geo-polymer	20 wt.% GO	100 S/m	[129]
	PBS	5 vol.% graphene	3.22×10^{-3} S/m	[85]
	DBP/PVB/EGB	50 wt.% graphene	71.5 S/m at RT 479.2 S/m at 450℃	[84]
	PTMC	0.5 wt.% graphene	$\sim1\times10^{-3}$ S/m	[122]
		1.5 wt.% graphene	$\sim1\times10^{-2}$ S/m	
		3 wt.% graphene	$\sim1\times10^{-1}$ S/m	
FDM	ABS	0.4 wt.% graphene	1.78×10^{-7} S/m	[110]
		2.3 wt.% graphene	3.04×10^{-7} S/m	
		3.8 wt.% graphene	6.4×10^{-5} S/m	
		5.6 wt.% graphene	1.05×10^{-3} S/m	
	ABS (chemical blending Process)	10 wt.% graphene	5.07 S/m	[168]
		25 wt.% graphene	7.29 S/m	
	ABS (mechanical blending Process)	10 wt.% graphene	3.63 S/m	
		25 wt.% graphene	4.85 S/m	
	PLA/PANI	10 wt.% graphene	14 S/m	[170]
	PETG/PANI	10 wt.% graphene	17 S/m	
	PMMA/PPY	10 wt.% graphene	1420 S/m	
SLS	PA	0.18 vol.% rGO	$4.97\ 10^{-7}$ S/m	[97]
		0.48 vol.% rGO	$2.33\ 10^{-6}$ S/m	
		0.72 vol.% rGO	$1.11\ 10^{-4}$ S/m	
		1.09 vol.% rGO	$1.46\ 10^{-3}$ S/m	
		3.83 vol.% rGO	$1.61\ 10^{-2}$ S/m	
		8.26 vol.% rGO	$1.25\ 10^{-1}$ S/m	
Novel 3D printer with a rolling tube and a sprayer	PCL	SLG	0.892 S/m	[192]
		MLG	0.637 S/m	

An *et al.* [193] developed a graphene aerogel based flexible sensor which had reversible mechanical deformation properties and great electrical conductivity using a GO ink via extrusion printing. Moreover, through suitable designs, human motion can be recognized by the printed graphene sensor which has potential for finger

motion manipulation auxiliary apparatuses (**Fig.14a-c**). Wu *et al.* [85] prepared an innovative self-healing conductive polymer composite ink based on PDMS using polyborosiloxane (PBS) with 5 vol.% graphene. Interestingly, PBS enabled the ink at the liquefied state which rapidly restored the solid-like state after being exposed to air. Based on these qualities, a chemical vapour sensor was prepared (**Fig.14d-f**). Manzanares *et al.* [113] reported PLA/graphene electrodes which could be promising as electrochemical sensors.

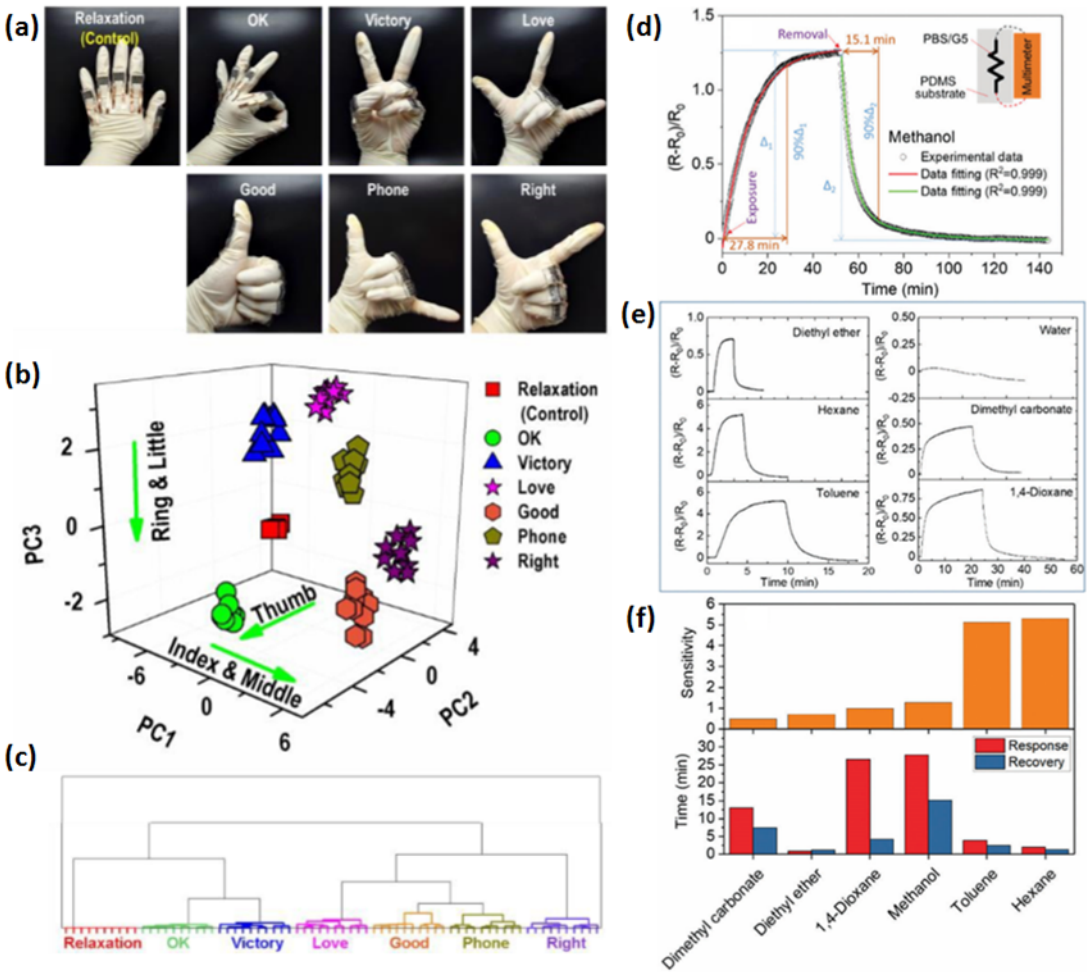

Fig. 14 Electronic discriminant analysis of seven gestures based on flexible graphene aerogel sensors and rational analysis. (a) Sensors placed on the finger joints, different gestures with the deformation degree of the sensors. (b) 3D representation of PCA result shows a clear clustering of the seven different gestures as analytes. (c) HCA gives the similarity clustering of the analytes based on the characteristic joints movement variation trend. Reprinted with permission from [193]. Copyright 2016 Royal Society of Chemistry. The normalized resistance response of the PBS/G5 sensor printed on the

PDMS substrate during the exposure to and removal from an atmosphere of chemical saturated vapour: (d) methanol and (e) various chemicals. The inset of (d) is the schematic illustration of the experimental set-up for measuring the resistance of the PBS/G5 sensor printed on the PDMS substrate. (f) The summarized performance of the PBS/G5 sensor for sensing various chemical vapours. Reprinted with permission from [85]. Copyright 2018 Royal Society of Chemistry.

Table 4 Graphene-modified polymers used in energy storage.

Application	AM method	Matrix	Effect	Refs
Lithium-ion batteries	FDM	LFP or LTO	Charging and discharging capacities of 117 and 91 mAh/g with good cycling stability	[188]
	FDM	PLA	A large mass of the active material available; high specific discharge capacity of 265 mAh/g with retention of 93% after 1000 cycles; good structural stability and high reversibility	[111]
	DIW	Sulphur copolymer/graphene	Exhibiting a high reversible capacity of 812,8 mAh/g and good cycle performance	[125]
Supercapacitors	DIW	SiO_2	1 mm electrodes with capacitance retention (ca. 90% from 0.5 to 10 A/g) and power densities (>4 kW/kg) that equal or exceed those of reported devices made with electrodes 10−100 times thinner	[119]
	FDM	PLA	High catalytic activity towards the hydrogen evolution reaction (−0.46 V vs. SCE) upon the 1000th cycle	[114]
Electrostatic discharge	FDM	Epoxy	Sheet resistance ranged from 0.67×10^2 to 8.2×10^3 Ω/sq.	[124]

5.3. Biocompatibility and Biomedical Applications

Recently, graphene-based polymeric materials have also attracted broad attention in biomedical applications. Advantages are not only the interesting electrical properties but also biocompatibility. Besides, the huge surface area of graphene can promote cellular interaction. When combining all those unique properties, graphene has great potential in tissue engineering, drug delivery, gene delivery and bioimaging, etc. Through suitable design, non-biodegradable graphene and its derivatives are able to degrade, for instance, GO was found to biodegrade by using hydrogen peroxide and horseradish peroxidase [194]. However, the biocompatibility mechanism of graphene

still remains largely unknown. Combining novel AM methods with GPMCs, numerous advantages can be achieved such as: a) controllable porosity, pore size, pore distribution and structure of the scaffold, leading to better bioactivity; b) GPMCs are flexible with excellent mechanical properties, enlarging its application area in both soft and hard tissue engineering; and c) the electrical conductivity of graphene can be used in biosensors and to detect *in-situ* cell signal response in living bodies. Biocompatibility properties such as biodegradation, non-cytotoxicity and gene expression performance of GPMCs are listed in **Table 5**.

Graphene, GO and other graphene related materials have been used as drug delivery [195, 196]. Meanwhile, they are beneficial for enhance cell growth and differentiation. Some biocompatible polymers with biomedical properties can be employed as cell supporting materials. One of the biomedical applications of GPMCs is in tissue engineering scaffolds. Huang *et al.* [123] dispersed graphene or GO into PU and printed the resulting materials as neural stem cell (NSC)-laden scaffolds for neural tissue regeneration. Besides, GPMCs can be used in bone tissue engineering applications for the substitution and regeneration of wounded tissues and organs. Kang *et al.* [197] developed a trachea scaffolds by using antibacterial patterned electrospun membranes and 3D printed TPU skeletons. GO was applied to enhance the antimicrobial ability of the electrospun membranes due to the damages to cell membranes of the microorganisms caused by the sharp edges of GO.

Qian *et al.* [192] integrated a novel 3D printing and layer-by-layer casting (LBLC) method to fabricate multi-layered porous nerve conduits. The resulting scaffold consisted of SLG/MLG and PCL, and resulted in precise control of quality, enhanced mechanical strength, eliminated random gaps between nanofibres and, most importantly, resulted in a homogeneous drug delivery. This innovative printer consisted of a rolling tube and a sprayer. A tubular mode with evenly distributed micro-needles was placed on a roller. The nozzle above this rolling tube directly sprayed different solutions on the rolling tube. The tube was rotating at a constant speed and added different layers to form a tubular structure (**Fig.15**). Obviously, polymers used in the biomedical area are biodegradable, biocompatible and non-cytotoxic, such as PCL, PEGDA, PLA etc. **Table 6** summarizes GPMCs produced by AM

studied in biomedical applications.

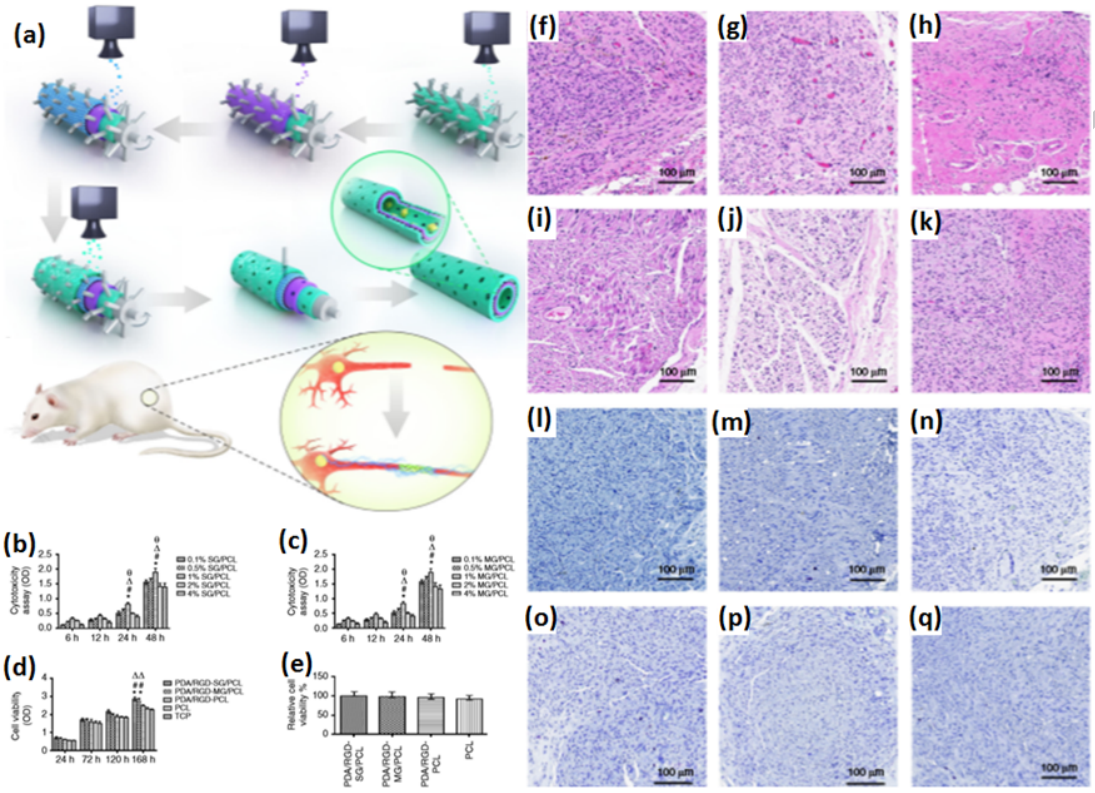

Fig. 15 (a) Schematic illustration of graphene-based nerve conduit fabrication with the LBLC method; (b) cytotoxicity assay for 0.1, 0.5, 1, 2.0, and 4.0 wt.% SG/PCL at different time points; (c) cytotoxicity assay for 0.1, 0.5, 1.0, 2.0 and 4.0 wt.% SG/PCL at different time points; (d) CCK8 assay for five groups; (e) relative cell viability by live and dead staining. Nerve regeneration at 18 weeks postoperatively. HE (f–k) and TB (i–q) staining for regenerated nerves at 18 weeks postoperatively. The scale bar is 100 μm. Reprinted with permission from [192]. Copyright 2018 Springer Nature.

Table 5 Biocompatibility of GPMCs

Cell types	Filler	Matrix	Biodegradation	Non-cytotoxicity	Gene expression	In vitro or in-vivo	Reference
MG-63	2.5 wt.% GO	PVA	√	√		In vitro	[96]
hMSCs	0-1 mg/ml GO	GelMA/PEGDA		√	Type II collagen, SOX-9 and aggrecan	In vitro	[108]
PC12 cells	1-5 wt.% graphene	PCL	√	√		In vitro	[120]
Human adipose-derived stem cells	(0.25, 0.50, and 0.75 wt.% graphene	PCL	√	√		In vitro	[156]
hMSCs	32, 56 ,75 wt.% graphene	PLG		√		In vitro and in-vivo	[121]
NIH3T3 mouse embryonic fibroblast cells	0-5 wt.% GO	TPU/PLA	√	√		In-vitro	[28]
Cell counting kit 8	0.1-4.0 wt.% graphene	PCL	√	√	Glial fibrillary acidic protein (GFAP), Class III β-tubulin (Tuj1), and S100	In-vitro and in-vivo	[192]
Mesenchymal stem cells	0.5, 1.5, 3.0 wt.% graphene	PTMC	√	√	ALP and Col I	In-vitro	[122]

Table 6 Composites fabricated via different AM techniques for tissue engineering.

Application	Technique	Category	Matrix	Effect	Refs
Hard tissue engineering	DIW	Bone	PCL	Enhancing cell viability/proliferation	[156]
	SLS	Bone	PVA	Enhancing human osteoblast-like MG-63 cells proliferation	[96]
	SLA	Cartilage	GelMA-PEGDA	Promoting chondrogenic differentiation	[108]
	Bioprinter	Cartilage	Collagen-chitosan	Benefiting to the proliferation of chondrocytes	[126]
Soft tissue engineering	Bioprinter	Neural tissue	PU	Enhancing the oxygen metabolism and the differentiation of neural stem cell	[123]
		Peripheral nerve restoration	PCL	Improving neural expression both in vitro and in vivo	[192]
	FDM	-	TPU/PLA	Enhancing in cellular growth	[28]
		Blood vessels/platelets	PCL/PCL-GR	Nontoxic graft for cell growth; drug-loaded	[115]
	DIW	Neural tissue	PLG	regeneration as single and multichannel nerve guide	[121]
		Mesenchymal stem cell	PTMC	Enhancing mesenchymal stem cell attachment and proliferation	[122]

5.4. Electromagnetic properties and Electromagnetic Interference Shielding

With the ever increasing density of emitters and electronic devices in our environment, it is critical to implement electromagnetic (EM) compatibility to avoid serious issues such as noise enhancement or faults of electronic equipment. That is to say, any new equipment must have adequate abilities to resist major disturbances, and coexist with multiple equipment [198]. Electrical conductivity, multilayers and absorbing capacity [112] of CNT/polymer, rGO/polymer and polymer/graphene composites have been investigated [198-200]. With the addition of graphene in polymer and adopting the FDM method, Viskadouraki *et al.* [200] enhanced the electrical conductivity of commercial polymeric materials (e.g., ABS and PLA), therefore improving their electromagnetic interference (EMI) shielding efficiency (EMI SE). PLA/graphene samples efficiently absorb up to 90% of the electromagnetic wave at the range of 3.5–7.0 GHz compared to that of 50% absorption for pure PLA. In future, it is believed that the performance of EMI SE will be improved by the optimization of 3D printing parameters,

functionally gradient structures and a combination of multifunctional nano/micro fillers (e.g., conductive and magnetic nanofillers). Through gradually varying the cellular structures of a single-phase material and a functionally graded structure (FGS) one can also achieve these multifunctional properties. Tian *et al.* [112] generated a rGO/PLA ultra-broadband EM wave absorber via FDM for metamaterial FGS with the integration of both good impedance matching and high microwave attenuation.

6. Current Challenges and Future Trends

AM is an effective method to manufacture graphene (or its derivatives) modified ceramic, metal or polymer composites with hierarchical micro- and macrostructures and multifunctional properties for applications in fields such as biocompatible electronic conductors, flexible sensors, etc. In comparison with conventional processing methods, AM is a one-step shaping technique (bottom-up method) which is more customizable and efficient for fabricating graphene-based composites, especially for complex geometries and internal porous structures. Graphene reinforced Al_2O_3 and polymer derived ceramic have been successfully fabricated via AM. Except for previously mentioned ceramics, other graphene-modified ceramic materials are still being explored for AM. To the best of our knowledge, only graphene reinforced iron, nickel, aluminium and copper have been manufactured via AM. These graphene-based metallic materials displayed good mechanical properties (e.g., fatigue life, vickers hardness and strength) while only few studies mentioned potential specific applications though. On the contrast, both AM techniques and composite preparation methods are well researched for polymer matrix composites. Owing to their low melting point and good processability, the majority of AM methods have however focused on polymer-based graphene composites among which FDM and DIW have been mostly used.

Currently, most of the work is restricted to laboratory research and only limited numbers of commercial products have been developed. One main hurdle for both GCMCs and GMMCs is that accuracy and low energy consumption cannot be obtained simultaneously. Because metal and ceramic materials have a fairly high melting point, laser-based AM methods with relatively high accuracy like SLS consume huge amounts of energy. Although the DIW method does not necessarily melt the materials, its accuracy is yet to improve for shaping ceramic and

metal materials. Future and novel developments in terms of good dispersion of graphene nanoplatelets, energy consumption and equipment will offer new opportunities for the use of AM printed GMMCs or GCMCs for different applications of functional technical parts. However, AM methods for polymers have demonstrated great capabilities, especially for SLA which can achieve high accuracy, high speed as well as has low energy consumption. However, it is worth noting that graphene can easily agglomerate in low viscosity UV-cured resin during the process of SLA. Therefore, suitable modification strategies for graphene should be designed to produce stable polymer/graphene mixtures.

Several factors may influence the quality of graphene-based composites: a) defects in the graphene sheet structure; b) homogenous and effective dispersion of high aspect-ratio graphene in a matrix; and c) selection and design of effective matrices suitable for both AM and the addition of graphene. The commercialization of graphene-based composites is still at an early stage of development and would need breakthroughs in the cost of good quality graphene dispersed in polymer as well as cost reduction of high precision 3D printing. The foundation of additive manufacturing high performance graphene-based composites: includes selection of materials (multi-materials), design of composition and structure (functionally graded composition and structure), online control or real time monitoring of 3D printing process (optimisation of printing parameters), interaction mechanisms and mathematical modelling, which will enable changes in precision/structure/property/functionality after printing.

AM is an inevitable trend for the future. The process allows for integration of multi structures and functions in a single component, introducing more controlled compositional and structural variations which are inaccessible via traditional processing methods. Owning to a tailored composition and structure, the resulting functionally graded materials and structures exhibit excellent multifunctional and unique properties, which can be implemented into various applications. Multi-materials can compensate individual shortcomings for each material and can lead to synergies. It is hence possible that graphene-based composites based on multi-material structures may achieve some exciting performances. The combination of AM and graphene-based composites opens new opportunities to solve issues for a wide range of applications such as metamaterial FGS for EMI and intelligent response materials implemented in a variety of sensors. Graphene-based composites via AM are still in their

infancy. However, it is envisioned that AM of high performance graphene-based composites can offer great potential for applications in especially the biomedical and electronic fields. In summary, the future development trends of 3D printing of graphene reinforced composites could have four main capabilities: high precision (micron-nanoscale), lightweight, multi-functionality and individual. To improve and maximize the potential applications of the 3D printed graphene reinforced composites, a large amount of multidisciplinary research needs to be conducted in the future.

Acknowledgments

The project was kindly supported by the Fundamental Research Funds for the Central Universities, China University of Geosciences (Wuhan) (No.CUG170677). The authors also gratefully acknowledge financial support from the National Natural Science Foundation of China (No. 51675496, No. 51671091) and Wuhan Applied Basic Research Project, China (No. 2017010201010126). We are grateful to Dr. Harshit Porwal for constructive reviews and many useful discussions.

Competing Interests

The authors declare that there is no conflict of interest regarding to the publication of this paper.

References

[1] Novoselov KS, Geim AK, Morozov SV, Jiang D, Zhang Y, Dubonos SV, et al. Electric Field Effect in Atomically Thin Carbon Films. Science. 2004;306(5696):666-9.
[2] Novoselov KS, Jiang Z, Zhang Y, Morozov SV, Stormer HL, Zeitler U, et al. Room-temperature quantum Hall effect in graphene. Science. 2007;315(5817):1379.
[3] Kan E, Li Z, Yang J. Graphene Nanoribbons: Geometric, Electronic, and Magnetic Properties: InTech; 2011. p. 331-48.
[4] Zhang L, Zhang F, Yang X, Long G, Wu Y, Zhang T, et al. Porous 3D graphene-based bulk materials with exceptional high surface area and excellent conductivity for supercapacitors. Sci Rep. 2013;3:1408.
[5] Geetha Bai R, Ninan N, Muthoosamy K, Manickam S. Graphene: A versatile platform for nanotheranostics and tissue engineering. Prog Mater Sci. 2018;91:24-69.
[6] Shin SR, Li YC, Jang HL, Khoshakhlagh P, Akbari M, Nasajpour A, et al. Graphene-based materials for tissue engineering. Adv Drug Deliv Rev. 2016;105(Part B):255-74.
[7] Balandin AA, Ghosh S, Bao W, Calizo I, Teweldebrhan D, Miao F, et al. Superior Thermal Conductivity of Single-Layer Graphene. Nano Lett. 2008;8(3):902-7.
[8] Nissimagoudar AS, Sankeshwar NS. Electronic thermal conductivity and thermopower of armchair graphene nanoribbons. Carbon. 2013;52:201-8.
[9] Ghosh S, Calizo I, Teweldebrhan D, Pokatilov EP, Nika DL, Balandin AA, et al. Extremely high thermal conductivity of graphene: Prospects for thermal management applications in nanoelectronic circuits. Appl Phys Lett. 2008;92(15):151911-3.
[10] Ye X-S, Shao Z-G, Zhao H, Yang L, Wang C-L. Intrinsic carrier mobility of germanene is larger than graphene's: first-principle calculations. RSC Adv. 2014;4(41):21216-20.
[11] Yoo BM, Shin HJ, Yoon HW, Park HB. Graphene and graphene oxide and their uses in barrier polymers. J. Appl Polym Sci. 2014;131(1):39628.
[12] Son DI, Kwon BW, Kim H-H, Park DH, Angadi B, Choi WK. Chemical exfoliation of pure graphene sheets from synthesized ZnO–graphene quasi core–shell quantum dots. Carbon. 2013;59:289-95.
[13] Poizot P, Humbert B, Ewels CP, Mevellec J-Y, Stephant N, Simonet J. Facile route to gold-graphene electrodes by exfoliation of natural graphite under electrochemical conditions. Carbon. 2016;107:823-30.
[14] Chen J, Duan M, Chen G. Continuous mechanical exfoliation of graphene sheets via three-roll mill. J Mater Chem. 2012;22(37):19625-8.
[15] Shin JH, Kim SH, Kwon SS, Park WI. Direct CVD growth of graphene on three-dimensionally-shaped dielectric substrates. Carbon. 2018;129:785-9.
[16] Ren F, Song D, Li Z, Jia L, Zhao Y, Yan D, et al. Synergistic effect of graphene nanosheets and carbonyl iron–nickel alloy hybrid filler on electromagnetic interference shielding and thermal conductivity of cyanate ester composites. J Mater Chem C. 2018;6(6):1476-86.
[17] Pavithra CL, Sarada BV, Rajulapati KV, Rao TN, Sundararajan G. A new electrochemical approach for the synthesis of copper-graphene nanocomposite foils with high hardness. Sci Rep. 2014;4:4049.
[18] Porwal H, Tatarko P, Grasso S, Khaliq J, Dlouhý I, Reece MJ. Graphene reinforced alumina nano-composites. Carbon. 2013;64:359-69.
[19] Kernin A, Wan K, Liu Y, Shi X, Kong J, Bilotti E, et al. The effect of graphene network formation on the electrical, mechanical, and multifunctional properties of graphene/epoxy nanocomposites. Compos Sci and Technol. 2019;169:224-31.
[20] Ma Y, Han J, Wang M, Chen X, Jia S. Electrophoretic deposition of graphene-based materials: A review of materials and their applications. J Mat. 2018;4(2):108-20.
[21] Chen L, Yu H, Zhong J, Wu J, Su W. Graphene based hybrid/composite for electron field emission: A review. J Alloys Compd. 2018;749:60-84.
[22] Lawal AT. Progress in utilisation of graphene for electrochemical biosensors. Biosens Bioelectron. 2018;106:149-78.

[23] Olszowska K, Pang J, Wrobel PS, Zhao L, Ta HQ, Liu Z, et al. Three-dimensional nanostructured graphene: Synthesis and energy, environmental and biomedical applications. Synth Met. 2017;234:53-85.
[24] Porwal H, Grasso S, Cordero-Arias L, Li C, Boccaccini AR, Reece MJ. Processing and bioactivity of 45S5 Bioglass-graphene nanoplatelets composites. J Mater Sci: Mater Med. 2014;25(6):1403-13.
[25] Tang D, Hao L, Li Y, Xiong W, Sun T, Yan X. Investigation of wax-based barite slurry and deposition for 3D printing landslide model. Compos Part A: Appl Sci Manuf. 2018;108:99-106.
[26] Veluru JB, Merum S, Radhamani AV, Doble M, Kumar TSS, Ramakrishna S. Additive manufacturing technologies: an overview of challenges and perspective of using electrospraying AU - Kiran, A. Sandeep Kranthi. Nanocomposites. 2019:1-25.
[27] Melchels FP, Feijen J, Grijpma DW. A poly($_{D,L}$-lactide) resin for the preparation of tissue engineering scaffolds by stereolithography. Biomaterials. 2009;30(23-24):3801-9.
[28] Chen Q, Mangadlao JD, Wallat J, De Leon A, Pokorski JK, Advincula RC. 3D Printing Biocompatible Polyurethane/Poly(lactic acid)/Graphene Oxide Nanocomposites: Anisotropic Properties. ACS Appl Mater Interfaces. 2017;9(4):4015-23.
[29] Porwal H, Saggar R. 6.6 Ceramic Matrix Nanocomposites. In: Beaumont PWR, Zweben CH, editors. Compr Compos Mater II. Oxford: Elsevier; 2018. p. 138-61.
[30] Shuai C, Feng P, Wu P, Liu Y, Liu X, Lai D, et al. A combined nanostructure constructed by graphene and boron nitride nanotubes reinforces ceramic scaffolds. Chem Eng J. 2017;313:487-97.
[31] Fan Y, Wang L, Li J, Li J, Sun S, Chen F, et al. Preparation and electrical properties of graphene nanosheet/Al2O3 composites. Carbon. 2010;48(6):1743-9.
[32] Lou Y, Liu G, Liu S, Shen J, Jin W. A facile way to prepare ceramic-supported graphene oxide composite membrane via silane-graft modification. Appl Surf Sci. 2014;307:631-7.
[33] Porwal H, Saggar R, Tatarko P, Grasso S, Saunders T, Dlouhý I, et al. Effect of lateral size of graphene nano-sheets on the mechanical properties and machinability of alumina nano-composites. Ceram Int. 2016;42(6):7533-42.
[34] Porwal H, Tatarko P, Grasso S, Hu C, Boccaccini AR, Dlouhý I, et al. Toughened and machinable glass matrix composites reinforced with graphene and graphene-oxide nano platelets. Sci Technol Adv Mater. 2013;14(5):055007.
[35] Porwal H, Tatarko P, Saggar R, Grasso S, Kumar Mani M, Dlouhý I, et al. Tribological properties of silica–graphene nano-platelet composites. Ceram Int. 2014;40(8, Part A):12067-74.
[36] Rahman A, Singh A, Karumuri S, Harimkar SP, Kalkan KA, Singh RP. Graphene Reinforced Silicon Carbide Nanocomposites: Processing and Properties: Spr Inte Publing; 2015. p. 165-76.
[37] Wang X, Lu M, Qiu L, Huang H, Li D, Wang H, et al. Graphene/titanium carbide composites prepared by sol–gel infiltration and spark plasma sintering. Ceram Int. 2016;42(1):122-31.
[38] Porwal H, Grasso S, Reece MJ. Review of graphene–ceramic matrix composites. Adv Appl Ceram. 2014;112(8):443-54.
[39] Mazo MA, Palencia C, Nistal A, Rubio F, Rubio J, Oteo JL. Dense bulk silicon oxycarbide glasses obtained by spark plasma sintering. J Eur Ceram Soc. 2012;32(12):3369-78.
[40] Zeng Z, Liu Y, Chen W, Li X, Zheng Q, Li K, et al. Fabrication and properties of in situ reduced graphene oxide-toughened zirconia composite ceramics. J Am Ceram Soc. 2018;101(8):3498-507.
[41] Inam F, Vo T, Bhat BR. Structural stability studies of graphene in sintered ceramic nanocomposites. Ceram Int. 2014;40(10):16227-33.
[42] Inam F, Heaton A, Brown P, Peijs T, Reece MJ. Effects of dispersion surfactants on the properties of ceramic–carbon nanotube (CNT) nanocomposites. Ceram Int. 2014;40(1):511-6.
[43] Inam F, Yan H, Peijs T, Reece MJ. The sintering and grain growth behaviour of ceramic–carbon nanotube nanocomposites. Compos Sci Technol. 2010;70(6):947-52.
[44] Yan H, Reece MJ, Peijs T. Structural and chemical stability of multiwall carbon nanotubes in sintered ceramic nanocomposite AU - Inam, F. Adv Appl Ceram. 2010;109(4):240-7.
[45] Porwal H, Grasso S, Mani MK, Reece MJ. In situ reduction of graphene oxide nanoplatelet during spark plasma sintering of a silica matrix composite. J Eur Ceram Soc.2014;34(14):3357-64.

[46] Shuai C, Gao C, Feng P, Peng S. Graphene-reinforced mechanical properties of calcium silicate scaffolds by laser sintering. RSC Adv. 2014;4(25):12782-8.
[47] Rashad M, Pan F, Asif M, Tang A. Powder metallurgy of Mg–1%Al–1%Sn alloy reinforced with low content of graphene nanoplatelets (GNPs). J Ind Eng Chem. 2014;20(6):4250-5.
[48] Khodabakhshi F, Nosko M, Gerlich AP. Effects of graphene nano-platelets (GNPs) on the microstructural characteristics and textural development of an Al-Mg alloy during friction-stir processing. Surf Coat Technol. 2018;335:288-305.
[49] Khodabakhshi F, Arab SM, Švec P, Gerlich AP. Fabrication of a new Al-Mg/graphene nanocomposite by multi-pass friction-stir processing: Dispersion, microstructure, stability, and strengthening. Mater Charact. 2017;132:92-107.
[50] Jeon C-H, Jeong Y-H, Seo J-J, Tien HN, Hong S-T, Yum Y-J, et al. Material properties of graphene/aluminum metal matrix composites fabricated by friction stir processing. Int J Precis Eng Man. 2014;15(6):1235-9.
[51] Zheng Y, Wang A, Cai W, Wang Z, Peng F, Liu Z, et al. Hydrothermal preparation of reduced graphene oxide–silver nanocomposite using Plectranthus amboinicus leaf extract and its electrochemical performance. Enzyme Microb Technol. 2016;95:112-7.
[52] Zhao C. Enhanced strength in reduced graphene oxide/nickel composites prepared by molecular-level mixing for structural applications. Appl Phys A: Mater Sci Process. 2015;118(2):409-16.
[53] Jaewon H, Taeshik Y, Sung Hwan J, Jinsup L, Taek-Soo K, Soon Hyung H, et al. Enhanced mechanical properties of graphene/copper nanocomposites using a molecular-level mixing process. Adv Mater. 2013;25(46):6724-9.
[54] Low CTJ, Wills RGA, Walsh FC. Electrodeposition of composite coatings containing nanoparticles in a metal deposit. Surf Coat Technol. 2006;201(1-2):371-83.
[55] Li J, An Z, Wang Z, Toda M, Ono T. Pulse-Reverse Electrodeposition and Micromachining of Graphene–Nickel Composite: An Efficient Strategy toward High-Performance Microsystem Application. ACS Appl Mater Interfaces. 2016;8(6):3969-76.
[56] Liu Y, Liu Y, Zhang Q, Zhang C, Wang J, Wu Y, et al. Control of the microstructure and mechanical properties of electrodeposited graphene/Ni composite. Mater Sci Eng: A. 2018;727:133-9.
[57] Li N, Zhang L, Xu M, Xia T, Ruan X, Song S, et al. Preparation and mechanical property of electrodeposited Al-graphene composite coating. Mater Des. 2016;111:522-7.
[58] Thiruvengadathan R, Chung SW, Basuray S, Balasubramanian B, Staley CS, Gangopadhyay K, et al. A Versatile Self-Assembly Approach toward High Performance Nanoenergetic Composite Using Functionalized Graphene. Langmuir. 2014;30(22):6556-64.
[59] Zan L, Xidan F, Qiang G, Lei Z, Genlian F, Zhiqiang L, et al. Graphene quality dominated interface deformation behavior of graphene-metal composite: the defective is better. Int J Plast. 2018;111: 253-65.
[60] Zan L, Qiang G, Zhiqiang L, Genlian F, Ding-Bang X, Yishi S, et al. Enhanced Mechanical Properties of Graphene (Reduced Graphene Oxide)/Aluminum Composites with a Bioinspired Nanolaminated Structure. Nano Lett. 2015;15(12):8077-83.
[61] Lin D, Richard Liu C, Cheng GJ. Single-layer graphene oxide reinforced metal matrix composites by laser sintering: Microstructure and mechanical property enhancement. Acta Mater. 2014;80:183-93.
[62] Kim H, Abdala AA, Macosko CW. Graphene/Polymer Nanocomposites. Macromolecules. 2010;43(16):6515-30.
[63] Verdejo R, Bernal MM, Romasanta LJ, Lopez-Manchado MA. Graphene filled polymer nanocomposites. J Mater Chem. 2011;21(10):3301-10.
[64] Singh V, Joung D, Zhai L, Das S, Khondaker SI, Seal S. Graphene based materials: Past, present and future. Prog Mater Sci. 2011;56(8):1178-271.
[65] Terrones M, Martín O, González M, Pozuelo J, Serrano B, Cabanelas JC, et al. Interphases in Graphene Polymer-based Nanocomposites: Achievements and Challenges. Adv Mater. 2011;23(44):5302-10.

[66] Kuilla T, Bhadra S, Yao D, Kim NH, Bose S, Lee JH. Recent advances in graphene based polymer composites. Prog Polym Sci. 2010;35(11):1350-75.
[67] Zhai Z, Zahabi H, Picot OT, Deng H, Fu Q, Bilotti E, et al. High mechanical reinforcing efficiency of layered poly(vinyl alcohol) – graphene oxide nanocomposites AU - Sellam, Charline. Nanocomposites. 2015;1(2):89-95.
[68] Hadavinia H, Zhang T, Liaghat G, Vahid S, Spacie C, Paton KR, et al. Improving the fracture toughness properties of epoxy using graphene nanoplatelets at low filler content AU - Domun, Nadiim. Nanocomposites. 2017;3(3):85-96.
[69] Zheng W, Lu X, Wong SC. Electrical and mechanical properties of expanded graphite-reinforced high-density polyethylene. Prog Polym Sci. 2010;91(5):2781-8.
[70] Liang J, Wang Y, Huang Y, Ma Y, Liu Z, Cai J, et al. Electromagnetic interference shielding of graphene/epoxy composites. Carbon. 2009;47(3):922-5.
[71] Chen G, Wu D, Weng W, Wu C. Exfoliation of graphite flake and its nanocomposites. Carbon. 2003;41(3):619-21.
[72] Xu Z, Gao C. In situPolymerization Approach to Graphene-Reinforced Nylon-6 Composites. Macromolecules. 2010;43(16):6716-23.
[73] Mohamadi S, Sharifi-Sanjani N. Investigation of the crystalline structure of PVDF in PVDF/PMMA/graphene polymer blend nanocomposites. Polym Compos. 2011;32(9):1451-60.
[74] Koo JH. Polymer nanocomposites: processing, characterization, and applications: McGraw-Hill; 2006; p. 61-74.
[75] Eriksson M, Goossens H, Peijs T. Influence of drying procedure on glass transition temperature of PMMA based nanocomposites. Nanocomposites. 2014;1(1):36-45.
[76] Wang XL, Huang WJ. Fabrication and Characterization of Graphene/Polyimide Nanocomposites. Adv Mater Res. 2013;785-786:138-144.
[77] Xu X-l, Yang C-j, Yang J-h, Huang T, Zhang N, Wang Y, et al. Excellent dielectric properties of poly(vinylidene fluoride) composites based on partially reduced graphene oxide. Compos Part B. 2017;109:91-100.
[78] Endoh M, Trojanowski R, Ramasamy RP, Gentleman MM, Butcher TA, Rafailovich MH. The thermo-mechanical response of PP nanocomposites at high graphene loading AU - Yang, Kai. Nanocomposites. 2015;1(3):126-37.
[79] Kim S, Do I, Drzal LT. Thermal stability and dynamic mechanical behavior of exfoliated graphite nanoplatelets-LLDPE nanocomposites. Polym Compos 2009;31(5):755-61.
[80] Chen G, Wu C, Weng W, Wu D, Yan W. Preparation of polystyrene/graphite nanosheet composite. Polymer. 2003;44(6):1781-4.
[81] Gao Y, Picot OT, Bilotti E, Peijs T. Influence of filler size on the properties of poly(lactic acid) (PLA)/graphene nanoplatelet (GNP) nanocomposites. Eur Polym J. 2017;86:117-31.
[82] Mohamadi S, Sharifi-Sanjani N. Crystallization of PVDF in graphene-filled electrospun PVDF/PMMA nanofibers processed at three different conditions. Fibers Polym. 2016;17(4):582-92.
[83] Araby S, Meng Q, Ma J. Electrical conductivity and mechanical performance of polymer/graphene composites developed by two compounding methods. In: Ye L, editor. Recent Advances in Structural Integrity Analysis - Proceedings of the International Congress (APCF/SIF-2014). Oxford: Woodhead Publishing; 2014. p. 370-4.
[84] Huang K, Yang J, Dong S, Feng Q, Zhang X, Ding Y, et al. Anisotropy of graphene scaffolds assembled by three-dimensional printing. Carbon. 2018;130:1-10.
[85] Wu T, Gray E, Chen B. A self-healing, adaptive and conductive polymer composite ink for 3D printing of gas sensors. J Mater Chem C. 2018;6(23):6200-7.
[86] Lin D, Jin S, Zhang F, Wang C, Wang Y, Zhou C, et al. 3D stereolithography printing of graphene oxide reinforced complex architectures. Nanotechnology. 2015;26(43):434003.
[87] Li X, Cai W, An J, Kim S, Nah J, Yang D, et al. Large-area synthesis of high-quality and uniform graphene films on copper foils. Science. 2009;324(5932):1312-4.

[88] Kaplas T, Kuzhir P. Ultra-thin Graphitic Film: Synthesis and Physical Properties. Nanoscale Res Lett. 2016;11(1):54.
[89] Xu C, Wang X, Zhu J. Graphene−Metal Particle Nanocomposites. J Phys Chem C 2008;112(50):19841-5.
[90] Standard A. ISO/ASTM 52900: 2015 Additive manufacturing-General principles-terminology. ASTM F2792-10e1. 2012.
[91] Bose S, Ke D, Sahasrabudhe H, Bandyopadhyay A. Additive manufacturing of biomaterials. Prog Mater Sci. 2018;93:45-111.
[92] Xiong W, Hao L, Li Y, Tang D, Cui Q, Feng Z, et al. Effect of selective laser melting parameters on morphology, microstructure, densification and mechanical properties of supersaturated silver alloy. Mater Des. 2019;170:107697.
[93] Zhou W, Dong M, Zhou Z, Sun X, Kikuchi K, Nomura N, et al. In situ formation of uniformly dispersed Al4C3 nanorods during additive manufacturing of graphene oxide/Al mixed powders. Carbon. 2019;141:67-75.
[94] Hu Z, Chen F, Xu J, Nian Q, Lin D, Chen C, et al. 3D printing graphene-aluminum nanocomposites. J Alloys Compd. 2018;746:269-76.
[95] Zengrong H, Feng C, Dong L, Qiong N, Pedram P, Xing Z, et al. Laser additive manufacturing bulk graphene–copper nanocomposites. Nanotechnology. 2017;28(44):445705.
[96] Shuai C, Feng P, Gao C, Shuai X, Xiao T, Peng S. Graphene oxide reinforced poly(vinyl alcohol): nanocomposite scaffolds for tissue engineering applications. RSC Adv. 2015;5(32):25416-23.
[97] de Leon AC, Rodier BJ, Bajamundi C, Espera A, Wei P, Kwon JG, et al. Plastic Metal-Free Electric Motor by 3D Printing of Graphene-Polyamide Powder. ACS Appl Energy Mater. 2018;1(4):1726-33.
[98] Hassanin H, Modica F, El-Sayed MA, Liu J, Essa K. Manufacturing of Ti-6Al-4V Micro-Implantable Parts Using Hybrid Selective Laser Melting and Micro-Electrical Discharge Machining. Adv Eng Mater. 2016;18(9):1544-9.
[99] Read N, Wang W, Essa K, Attallah MM. Selective laser melting of AlSi10Mg alloy: Process optimisation and mechanical properties development. Mater Des. 2015;65:417-24.
[100] Carter LN, Essa K, Attallah MM. Optimisation of selective laser melting for a high temperature Ni-superalloy. RAPID PROTOTYPING J. 2015;21(4):423-32.
[101] Carter LN, Wang X, Read N, Khan R, Aristizabal M, Essa K, et al. Process optimisation of selective laser melting using energy density model for nickel based superalloys. Mater Sci Technol. 2016;32(7):657-61.
[102] Moroni L, Boland T, Burdick JA, De Maria C, Derby B, Forgacs G, et al. Biofabrication: A Guide to Technology and Terminology. Trends Biotechnol. 2018;36(4):384-402.
[103] Gibson I, Rosen D, Stucker B. Vat Photopolymerization Processes. In: Gibson I, Rosen D, Stucker B, editors. Additive Manufacturing Technologies: 3D Printing, Rapid Prototyping, and Direct Digital Manufacturing. New York, NY: Springer New York; 2015. p. 63-106.
[104] Melchels FP, Feijen J, Grijpma DW. A review on stereolithography and its applications in biomedical engineering. Biomaterials. 2010;31(24):6121-30.
[105] Korhonen H, Sinh LH, Luong ND, Lehtinen P, Verho T, Partanen J, et al. Fabrication of graphene-based 3D structures by stereolithography. Phys Status Solidi A. 2016;213(4):982-5.
[106] Li J, Wang L, Dai L, Zhong L, Liu B, Ren J, et al. Synthesis and characterization of reinforced acrylate photosensitive resin by 2-hydroxyethyl methacrylate-functionalized graphene nanosheets for 3D printing. J Mater Sci 2017;53(3):1874-86.
[107] Manapat JZ, Mangadlao JD, Tiu BD, Tritchler GC, Advincula RC. High-Strength Stereolithographic 3D Printed Nanocomposites: Graphene Oxide Metastability. ACS Appl Mater Interfaces. 2017;9(11):10085-93.
[108] Zhou X, Nowicki M, Cui H, Zhu W, Fang X, Miao S, et al. 3D bioprinted graphene oxide-incorporated matrix for promoting chondrogenic differentiation of human bone marrow mesenchymal stem cells. Carbon. 2017;116:615-24.

[109] Ngo TD, Kashani A, Imbalzano G, Nguyen KTQ, Hui D. Additive manufacturing (3D printing): A review of materials, methods, applications and challenges. Compos Part B: Eng. 2018;143:172-96.
[110] Wei X, Li D, Jiang W, Gu Z, Wang X, Zhang Z, et al. 3D Printable Graphene Composite. Sci Rep. 2015;5:11181.
[111] Vernardou D, Vasilopoulos KC, Kenanakis G. 3D printed graphene-based electrodes with high electrochemical performance. Appl Phys A: Mater Sci. Process. 2017;123(10):623.
[112] Yin L, Tian X, Shang Z, Li D. Ultra-broadband metamaterial absorber with graphene composites fabricated by 3D printing. Mater Lett. 2019;239:132-5.
[113] Manzanares Palenzuela CL, Novotny F, Krupicka P, Sofer Z, Pumera M. 3D-Printed Graphene/Polylactic Acid Electrodes Promise High Sensitivity in Electroanalysis. Anal Chem. 2018;90(9):5753-7.
[114] Foster CW, Down MP, Zhang Y, Ji X, Rowley-Neale SJ, Smith GC, et al. 3D Printed Graphene Based Energy Storage Devices. Sci Rep. 2017;7:42233.
[115] Misra SK, Ostadhossein F, Babu R, Kus J, Tankasala D, Sutrisno A, et al. 3D-Printed Multidrug-Eluting Stent from Graphene-Nanoplatelet-Doped Biodegradable Polymer Composite. Adv Healthcare Mater. 2017;6(11):1700008.
[116] Wang J, Liu Y, Fan Z, Wang W, Wang B, Guo Z. Ink-based 3D printing technologies for graphene-based materials: a review. Adv Compos Hybrid Mater. 2019;2(1):1-33.
[117] Garcia-Tunon E, Barg S, Franco J, Bell R, Eslava S, D'Elia E, et al. Printing in three dimensions with graphene. Adv Mater. 2015;27(10):1688-93.
[118] Zhu C, Han TY, Duoss EB, Golobic AM, Kuntz JD, Spadaccini CM, et al. Highly compressible 3D periodic graphene aerogel microlattices. Nat Commun. 2015;6:6962.
[119] Zhu C, Liu T, Qian F, Han TY, Duoss EB, Kuntz JD, et al. Supercapacitors Based on Three-Dimensional Hierarchical Graphene Aerogels with Periodic Macropores. Nano Lett. 2016;16(6):3448-56.
[120] Sayyar S, Cornock R, Murray E, Beirne S, Officer DL, Wallace GG. Extrusion Printed Graphene/Polycaprolactone/Composites for Tissue Engineering. Mater Sci Forum. 2013;773-774:496-502.
[121] Jakus AE, Secor EB, Rutz AL, Jordan SW, Hersam MC, Shah RN. Three-dimensional printing of high-content graphene scaffolds for electronic and biomedical applications. ACS Nano. 2015;9(4):4636-48.
[122] Sayyar S, Bjorninen M, Haimi S, Miettinen S, Gilmore K, Grijpma D, et al. UV Cross-Linkable Graphene/Poly(trimethylene Carbonate) Composites for 3D Printing of Electrically Conductive Scaffolds. ACS Appl Mater Interfaces. 2016;8(46):31916-25.
[123] Huang C-T, Kumar Shrestha L, Ariga K, Hsu S-h. A graphene–polyurethane composite hydrogel as a potential bioink for 3D bioprinting and differentiation of neural stem cells. J Mater Chem B. 2017;5(44):8854-64.
[124] Compton BG, Hmeidat NS, Pack RC, Heres MF, Sangoro JR. Electrical and Mechanical Properties of 3D-Printed Graphene-Reinforced Epoxy. JOM. 2017;70(3):292-7.
[125] Shen K, Mei H, Li B, Ding J, Yang S. 3D Printing Sulfur Copolymer-Graphene Architectures for Li-S Batteries. Adv Energy Mater. 2018;8(4):1701527.
[126] Cheng Z, Landish B, Chi Z, Nannan C, Jingyu D, Sen L, et al. 3D printing hydrogel with graphene oxide is functional in cartilage protection by influencing the signal pathway of Rank/Rankl/OPG. Mater Sci Eng C. 2018;82:244-52.
[127] Tubío CR, Rama A, Gómez M, del Río F, Guitián F, Gil A. 3D-printed graphene-Al2O3 composites with complex mesoscale architecture. Ceram Int. 2018;44(5):5760-7.
[128] Jakus AE, Shah RN. Multi and mixed 3D-printing of graphene-hydroxyapatite hybrid materials for complex tissue engineering. J Biomed Mater Res A. 2017;105(1):274-83.
[129] Zhong J, Zhou G-X, He P-G, Yang Z-H, Jia D-C. 3D printing strong and conductive geo-polymer nanocomposite structures modified by graphene oxide. Carbon. 2017;117:421-6.

[130] Ladd C, So JH, Muth J, Dickey MD. 3D printing of free standing liquid metal microstructures. Adv Mater. 2013;25(36):5081-5.
[131] Shirazi SF, Gharehkhani S, Mehrali M, Yarmand H, Metselaar HS, Adib Kadri N, et al. A review on powder-based additive manufacturing for tissue engineering: selective laser sintering and inkjet 3D printing. Sci. Technol. Adv Mater. 2015;16(3):033502.
[132] de Leon AC, Chen Q, Palaganas NB, Palaganas JO, Manapat J, Advincula RC. High performance polymer nanocomposites for additive manufacturing applications. React Funct Polym. 2016;103:141-55.
[133] Azhari A, Marzbanrad E, Yilman D, Toyserkani E, Pope MA. Binder-jet powder-bed additive manufacturing (3D printing) of thick graphene-based electrodes. Carbon. 2017;119:257-66.
[134] Mohan VB, Lau K-t, Hui D, Bhattacharyya D. Graphene-based materials and their composites: A review on production, applications and product limitations. Compos Part B: Eng. 2018;142:200-20.
[135] Khalil I, Rahmati S, Muhd Julkapli N, Yehye WA. Graphene metal nanocomposites — Recent progress in electrochemical biosensing applications. J Ind Eng Chem. 2018;59:425-39.
[136] Wang C, Astruc D. Recent developments of metallic nanoparticle-graphene nanocatalysts. Prog. Mater Sci. 2018;94:306-83.
[137] Liu J, Choi HJ, Meng L-Y. A review of approaches for the design of high-performance metal/graphene electrocatalysts for fuel cell applications. J Ind Eng Chem. 2018;64:1-15.
[138] Idowu A, Boesl B, Agarwal A. 3D graphene foam-reinforced polymer composites – A review. Carbon. 2018;135:52-71.
[139] Mittal G, Dhand V, Rhee KY, Park S-J, Lee WR. A review on carbon nanotubes and graphene as fillers in reinforced polymer nanocomposites. J Ind Eng Chem. 2015;21:11-25.
[140] Murayama N, Hirao K, Sando M, Tsuchiya T, Yamaguchi H. High-temperature electro-ceramics and their application to SiC power modules. Ceram Int. 2018;44(4):3523-30.
[141] Picot OT, Rocha VG, Ferraro C, Ni N, D'Elia E, Meille S, et al. Using graphene networks to build bioinspired self-monitoring ceramics. Nat Commun. 2017;8:14425.
[142] Wu C, Xia L, Han P, Xu M, Fang B, Wang J, et al. Graphene-oxide-modified β-tricalcium phosphate bioceramics stimulate in vitro and in vivo osteogenesis. Carbon. 2015;93:116-29.
[143] Zhang Y, Zhai D, Xu M, Yao Q, Chang J, Wu C. 3D-printed bioceramic scaffolds with a Fe3O4/graphene oxide nanocomposite interface for hyperthermia therapy of bone tumor cells. J Mater Chem B. 2016;4(17):2874-86.
[144] Colombo P, Mera G, Riedel R, Sorarù GD. Polymer-Derived Ceramics: 40 Years of Research and Innovation in Advanced Ceramics. J Am Ceram Soc. 2010,93(7):1805-37.
[145] Li S, Duan W, Zhao T, Han W, Wang L, Dou R, et al. The fabrication of SiBCN ceramic components from preceramic polymers by digital light processing (DLP) 3D printing technology. J Eur Ceram Soc. 2018;38(14):4597-603.
[146] Pierin G, Grotta C, Colombo P, Mattevi C. Direct Ink Writing of micrometric SiOC ceramic structures using a preceramic polymer. J Eur Ceram Soc. 2016;36(7):1589-94.
[147] Zhang N, Molenda JA, Fournelle JH, Murphy WL, Sahai N. Effects of pseudowollastonite ($CaSiO_3$) bioceramic on in vitro activity of human mesenchymal stem cells. Biomaterials. 2010;31(30):7653-65.
[148] Wang C, Xue Y, Lin K, Lu J, Chang J, Sun J. The enhancement of bone regeneration by a combination of osteoconductivity and osteostimulation using β-$CaSiO_3$/β-$Ca_3(PO_4)_2$ composite bioceramics. Acta Biomater. 2012;8(1):350-60.
[149] Raj V, Raj RM, Sasireka A, Priya P. Fabrication of TiO_2-strontium loaded $CaSiO_3$/biopolymer coatings with enhanced biocompatibility and corrosion resistance by controlled release of minerals for improved orthopedic applications. J Mech Behav Biomed Mater. 2016;60:476-91.
[150] Gupta Chatterjee S, Chatterjee S, Ray AK, Chakraborty AK. Graphene–metal oxide nanohybrids for toxic gas sensor: A review. Sens Actuators B. 2015;221:1170-81.
[151] Majeed A, Ullah W, Anwar AW, Nasreen F, Sharif A, Mustafa G, et al. Graphene-metal oxides/hydroxide nanocomposite materials: Fabrication advancements and supercapacitive performance. J Alloys Compd. 2016;671:1-10.

[152] Lin D, Motlag M, Saei M, Jin S, Rahimi RM, Bahr D, et al. Shock engineering the additive manufactured graphene-metal nanocomposite with high density nanotwins and dislocations for ultra-stable mechanical properties. Acta Mater. 2018;150:360-72.
[153] Wang Y, Shi J, Lu S, Wang Y. Selective Laser Melting of Graphene-Reinforced Inconel 718 Superalloy: Evaluation of Microstructure and Tensile Performance. J MANUF SCI E. 2016;139(4):041005.
[154] Laha T, Kuchibhatla S, Seal S, Li W, Agarwal A. Interfacial phenomena in thermally sprayed multiwalled carbon nanotube reinforced aluminum nanocomposite. Acta Mater. 2007;55(3):1059-66.
[155] Bustillos J, Montero D, Nautiyal P, Loganathan A, Boesl B, Agarwal A. Integration of graphene in poly(lactic) acid by 3D printing to develop creep and wear-resistant hierarchical nanocomposites. Polym Compos. 2017. Polym Compos. 2017,39:3877-88.
[156] Wang W, Caetano G, Ambler WS, Blaker JJ, Frade MA, Mandal P, et al. Enhancing the Hydrophilicity and Cell Attachment of 3D Printed PCL/Graphene Scaffolds for Bone Tissue Engineering. Materials. 2016;9(12):992.
[157] Angjellari M, Tamburri E, Montaina L, Natali M, Passeri D, Rossi M, et al. Beyond the concepts of nanocomposite and 3D printing: PVA and nanodiamonds for layer-by-layer additive manufacturing. Mater Des. 2017;119:12-21.
[158] Miller AT, Safranski DL, Smith KE, Sycks DG, Guldberg RE, Gall K. Fatigue of injection molded and 3D printed polycarbonate urethane in solution. Polymer. 2017;108:121-34.
[159] Wang X, Jiang M, Zhou Z, Gou J, Hui D. 3D printing of polymer matrix composites: A review and prospective. Compos Part B: Eng. 2017;110:442-58.
[160] Li Y, Zhang H, Liu Y, Wang H, Huang Z, Peijs T, et al. Synergistic effects of spray-coated hybrid carbon nanoparticles for enhanced electrical and thermal surface conductivity of CFRP laminates. Compos Part A: Appl Sci Manuf. 2018;105:9-18.
[161] Li Y, Zhang H, Porwal H, Huang Z, Bilotti E, Peijs T. Mechanical, electrical and thermal properties of in-situ exfoliated graphene/epoxy nanocomposites. Compos Part A: Appl Sci Manuf. 2017;95:229-36.
[162] Li Y, Zhang H, Crespo M, Porwal H, Picot O, Santagiuliana G, et al. In Situ Exfoliation of Graphene in Epoxy Resins: A Facile Strategy to Efficient and Large Scale Graphene Nanocomposites. ACS Appl Mater Interfaces. 2016;8(36):24112-22.
[163] Prolongo SG, Jimenez-Suarez A, Moriche R, Ureña A. In situ processing of epoxy composites reinforced with graphene nanoplatelets. Compos Sci Technol. 2013;86:185-91.
[164] Zeng C, Lu S, Xiao X, Gao J, Pan L, He Z, et al. Enhanced thermal and mechanical properties of epoxy composites by mixing noncovalently functionalized graphene sheets. Polym Bull. 2014;72(3):453-72.
[165] Liu Y, Wu H, Chen G. Enhanced mechanical properties of nanocomposites at low graphene content based onin situball milling. Polym Compos. 2016;37(4):1190-7.
[166] Santagiuliana G, Picot OT, Crespo M, Porwal H, Zhang H, Li Y, et al. Breaking the Nanoparticle Loading–Dispersion Dichotomy in Polymer Nanocomposites with the Art of Croissant-Making. ACS Nano. 2018;12(9):9040-50.
[167] Dul S, Fambri L, Pegoretti A. Fused deposition modelling with ABS–graphene nanocomposites. Compos Part A: Appl Sci Manuf. 2016;85:181-91.
[168] Singh R, Sandhu GS, Penna R, Farina I. Investigations for Thermal and Electrical Conductivity of ABS-Graphene Blended Prototypes. Materials. 2017;10(8):881.
[169] Gnanasekaran K, Heijmans T, van Bennekom S, Woldhuis H, Wijnia S, de With G, et al. 3D printing of CNT- and graphene-based conductive polymer nanocomposites by fused deposition modeling. Appl Mater Today. 2017;9:21-8.
[170] Mohan VB, Krebs BJ, Bhattacharyya D. Development of novel highly conductive 3D printable hybrid polymer-graphene composites. Mater Today Commun. 2018;17:554-61.
[171] Wang D, Huang X, Li J, He B, Liu Q, Hu L, et al. 3D printing of graphene-doped target for "matrix-free" laser desorption/ionization mass spectrometry. Chem Commun. 2018;54(22):2723-6.

[172] Lim SM, Shin BS, Kim K. Characterization of Products Using Additive Manufacturing with Graphene/Photopolymer-Resin Nano-Fluid. J Nanosci Nanotechnol. 2017;17(8):5492-5.
[173] Feng Z, Li Y, Hao L, Yang Y, Tang T, Tang D, et al. Graphene-Reinforced Biodegradable Resin Composites for Stereolithographic 3D Printing of Bone Structure Scaffolds. J Nanomater. 2019;2019:1-13.
[174] Hensleigh RM, Cui H, Oakdale JS, Ye JC, Campbell PG, Duoss EB, et al. Additive manufacturing of complex micro-architected graphene aerogels. Mater Horiz. 2018;5(6):1035-41.
[175] Gao Y, Picot OT, Tu W, Bilotti E, Peijs T. Multilayer coextrusion of graphene polymer nanocomposites with enhanced structural organization and properties. J Appl Polym Sci. 2018;135(13):46041.
[176] Stankovich S, Dikin DA, Dommett GH, Kohlhaas KM, Zimney EJ, Stach EA, et al. Graphene-based composite materials. Nature. 2006;442(7100):282-6.
[177] Feng Z, Li Y, Xin C, Tang D, Xiong W, Zhang H. Fabrication of Graphene-Reinforced Nanocomposites with Improved Fracture Toughness in Net Shape for Complex 3D Structures via Digital Light Processing. C. 2019;5(2):25.
[178] Huang K, Dong S, Yang J, Yan J, Xue Y, You X, et al. Three-dimensional printing of a tunable graphene-based elastomer for strain sensors with ultrahigh sensitivity. Carbon. 2019;143:63-72.
[179] Terrones M, Martín O, González M, Pozuelo J, Serrano B, Cabanelas JC, et al. Interphases in Graphene Polymer-based Nanocomposites: Achievements and Challenges. Adv Mater. 2011;23(44):5302-10.
[180] Moon IK, Lee J, Ruoff RS, Lee H. Reduced graphene oxide by chemical graphitization. Nat Commun. 2010;1:73.
[181] Compton OC, Dikin DA, Putz KW, Brinson LC, Nguyen ST. Electrically conductive "alkylated" graphene paper via chemical reduction of amine-functionalized graphene oxide paper. Adv Mater. 2010;22(8):892-6.
[182] Eda G, Chhowalla M. Graphene-based Composite Thin Films for Electronics. Nano Lett. 2009;9(2):814.
[183] M. Zhang S, Lin L, Deng H, Gao X, Bilotti E, Peijs T, et al. Synergistic effect in conductive networks constructed with carbon nanofillers in different dimensions. Express Polymer Lett. 2012,6:159-168.
[184] Foygel M, Morris RD, Anez D, French S, Sobolev VL. Theoretical and computational studies of carbon nanotube composites and suspensions: Electrical and thermal conductivity. Phys Rev B. 2005,71(10):104201.
[185] Hicks J, Behnam A, Ural A. A computational study of tunneling-percolation electrical transport in graphene-based nanocomposites. Appl Phys Lett. 2009;95(21):282.
[186] Zhang R, Baxendale M, Peijs T. Universal resistivity–strain dependence of carbon nanotube/polymer composites. Phys Rev B: Condens Matter Mater Phys. 2007;76(19):195433.
[187] Gao Y, Picot OT, Zhang H, Bilotti E, Peijs T. Synergistic effects of filler size on thermal annealing-induced percolation in polylactic acid (PLA)/graphite nanoplatelet (GNP) nanocomposites. Nanocomposites. 2017;3(2):67-75.
[188] Fu K, Wang Y, Yan C, Yao Y, Chen Y, Dai J, et al. Graphene Oxide-Based Electrode Inks for 3D-Printed Lithium-Ion Batteries. Adv Mater. 2016;28(13):2587-94.
[189] Santra S, Hu G, Howe RC, De Luca A, Ali SZ, Udrea F, et al. CMOS integration of inkjet-printed graphene for humidity sensing. Sci Rep. 2015;5:17374.
[190] Bollella P, Fusco G, Tortolini C, Sanzo G, Favero G, Gorton L, et al. Beyond graphene: Electrochemical sensors and biosensors for biomarkers detection. Biosens Bioelectron. 2017;89:152-66
[191] Vlasceanu GM, Amarandi RM, Ionita M, Tite T, Iovu H, Pilan L, et al. Versatile graphene biosensors for enhancing human cell therapy. Biosens Bioelectron. 2018;117:283-302.
[192] Qian Y, Zhao X, Han Q, Chen W, Li H, Yuan W. An integrated multi-layer 3D-fabrication of PDA/RGD coated graphene loaded PCL nanoscaffold for peripheral nerve restoration. Nat Commun. 2018;9(1):323.

[193] An B, Ma Y, Li W, Su M, Li F, Song Y. Three-dimensional multi-recognition flexible wearable sensor via graphene aerogel printing. Chem Commun. 2016;52(73):10948-51.
[194] Kotchey GP, Allen BL, Vedala H, Yanamala N, Kapralov AA, Tyurina YY, et al. The enzymatic oxidation of graphene oxide. ACS Nano. 2011;5(3):2098-108.
[195] Zhang Q, Wu Z, Li N, Pu Y, Wang B, Zhang T, et al. Advanced review of graphene-based nanomaterials in drug delivery systems: Synthesis, modification, toxicity and application. Mater Sci Eng C. 2017;77:1363-75.
[196] Liu J, Dong J, Zhang T, Peng Q. Graphene-based nanomaterials and their potentials in advanced drug delivery and cancer therapy. J Control Release. 2018;286:64-73.
[197] Kang Y, Wang C, Qiao Y, Gu J, Zhang H, Peijs T, et al. Tissue-Engineered Trachea Consisting of Electrospun Patterned sc-PLA/GO- g-IL Fibrous Membranes with Antibacterial Property and 3D-Printed Skeletons with Elasticity. Biomacromolecules. 2019;20(4):1765-76.
[198] Prashantha K, Roger F. Multifunctional properties of 3D printed poly(lactic acid)/graphene nanocomposites by fused deposition modeling. J Macromol Sci A. 2016;54(1):24-9.
[199] Paddubskaya A, Valynets N, Kuzhir P, Batrakov K, Maksimenko S, Kotsilkova R, et al. Electromagnetic and thermal properties of three-dimensional printed multilayered nano-carbon/poly(lactic) acid structures. J Appl Phys. 2016;119(13):135102.
[200] Viskadourakis Z, Vasilopoulos KC, Economou EN, Soukoulis CM, Kenanakis G. Electromagnetic shielding effectiveness of 3D printed polymer composites. Appl Phys A: Mater Sci Process. 2017;123(12):736